

Review

Spatial profiling technologies illuminate the tumor microenvironment

Ofer Elhanani,^{1,2} Raz Ben-Uri,^{1,2} and Leeat Keren^{1,*}

¹Department of Molecular Cell Biology, Weizmann Institute of Science, Rehovot, Israel

²These authors contributed equally

*Correspondence: leeat.keren@weizmann.ac.il

<https://doi.org/10.1016/j.ccr.2023.01.010>

SUMMARY

The tumor microenvironment (TME) is composed of many different cellular and acellular components that together drive tumor growth, invasion, metastasis, and response to therapies. Increasing realization of the significance of the TME in cancer biology has shifted cancer research from a cancer-centric model to one that considers the TME as a whole. Recent technological advancements in spatial profiling methodologies provide a systematic view and illuminate the physical localization of the components of the TME. In this review, we provide an overview of major spatial profiling technologies. We present the types of information that can be extracted from these data and describe their applications, findings and challenges in cancer research. Finally, we provide a future perspective of how spatial profiling could be integrated into cancer research to improve patient diagnosis, prognosis, stratification to treatment and development of novel therapeutics.

The tumor microenvironment is composed of many different cell types, including malignant cells, but also non-transformed cells, such as fibroblasts, immune cells, neurons, lymphatics and vasculature. Each of these cell types can further assume a variety of phenotypes, defined by co-expression of multiple proteins. These cells organize in spatially structured arrangements, exhibiting microenvironmental niches, nutrient gradients and cell-cell interactions. In recent years, it has become increasingly appreciated that this ecosystem, collectively termed the tumor microenvironment, plays a crucial role in mediating complex phenomena, such as tumor progression and response to treatment.^{1,2}

Recent technological advancements in spatial profiling methodologies hold promise to capture the complexity of the TME. These methodologies allow gauging the expression of a multitude of proteins and transcripts in tissue specimens while preserving tissue architecture. In the last decade, we have witnessed a continuous maturation of these modalities, reducing costs and handling time, while increasing spatial and molecular resolutions, making them ready for implementation to cancer research. In this review, we provide an overview of technologies for spatial transcriptomic and proteomic profiling of tissues. We discuss the types of extracted information that these technologies yield and describe their application, key findings, and challenges in the field of cancer. Finally, we provide a future perspective on spatial profiling in cancer, describing new avenues expected to be explored in the next few years that will allow integrating spatial information into improving patient diagnosis, prognosis, stratification to treatments, and development of new drugs.

A SUITE OF SPATIAL PROFILING TECHNOLOGIES

In the past decade a suite of technologies to measure the genome,^{3–10} transcriptome,^{11–16} proteome,^{17,18} and metabo-

lome^{19–22} *in situ* have been developed and have also been reviewed in detail elsewhere.^{23–30} For the purpose of this review, we collectively refer to these as spatial profiling technologies. Here, we focus on two major modalities for spatial profiling: (1) methods for spatial measurements of messenger RNAs (mRNAs) and (2) antibody-based methods to measure proteins *in situ*. To conform with common nomenclature of these technologies in the literature, we refer to the former as *spatial transcriptomics* and the latter as *multiplexed imaging*, even though these names may not always accurately reflect the underlying technologies.

SPATIAL MEASUREMENTS OF mRNAs (SPATIAL TRANSCRIPTOMICS)

Although there are many spatially resolved transcriptomic methods, they can generally be divided into two major groups according to their detection strategies. Most spatial transcriptomic techniques use either a spatial indexing or imaging-based approaches to measure and quantify mRNA molecules *in situ*.

Spatial indexing approaches

Spatial indexing approaches use local hybridization of barcodes to RNA molecules, followed by quantification of gene expression profiles using next-generation sequencing (Figure 1A). Briefly, an array containing clusters of unique barcoded oligo(dT) primers (spots) is covered with a tissue section. Tissue permeabilization allows native RNA molecules to diffuse from the tissue to the array and hybridize with these barcodes. The RNA molecules then undergo cDNA synthesis directly on the slide followed by tissue digestion and removal. cDNA fragments are pooled and sequenced along with their attached barcodes to generate gene expression profiles that can be mapped back to their spatial coordinates using the barcodes, thus retaining spatial



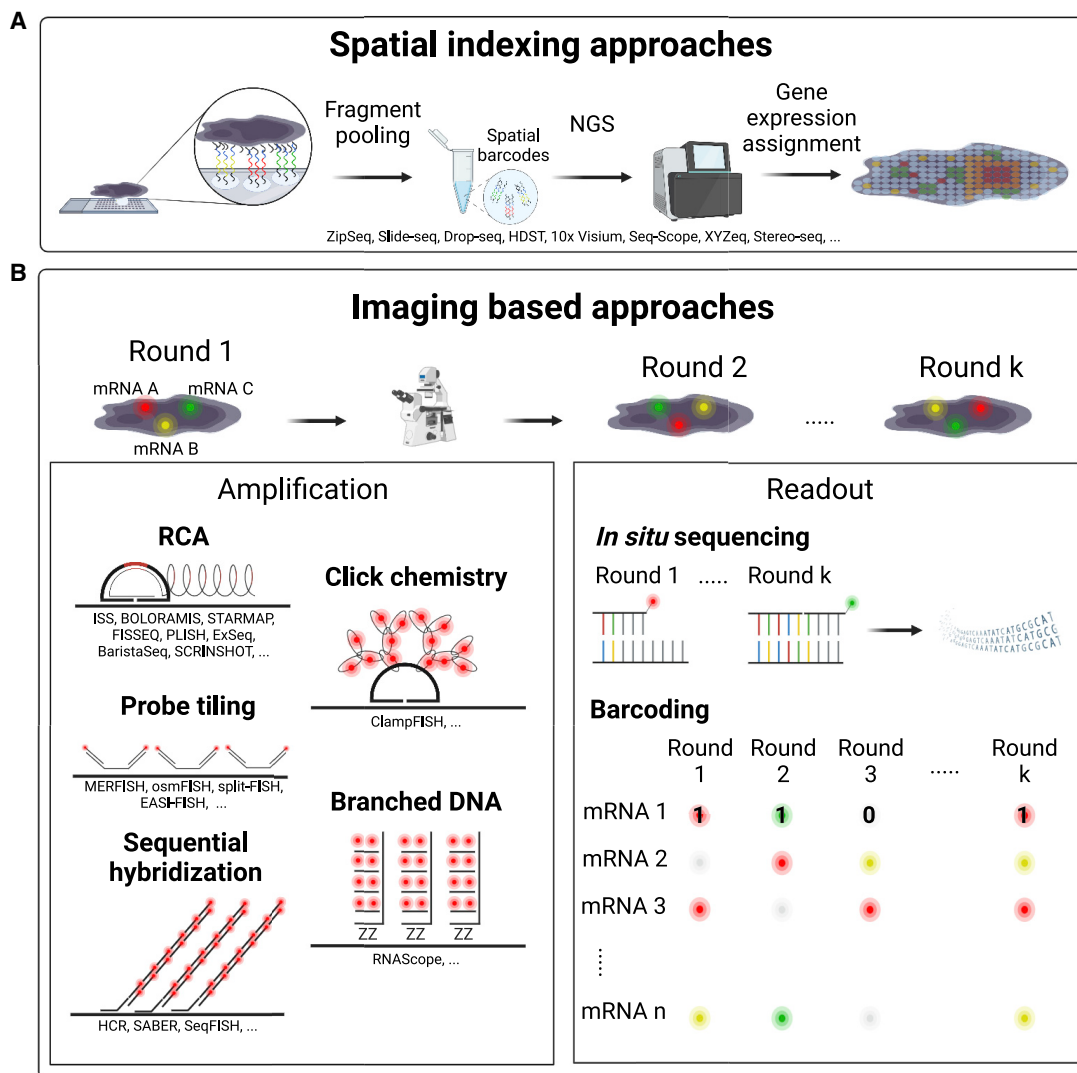


Figure 1. Technologies for spatial profiling of mRNA

(A) Spatial indexing methods perform hybridization of RNAs to barcoded capture arrays, followed by fragment pooling and sequencing. The barcodes make it possible to map transcripts to their spatial positions.

(B) Imaging-based methods generate optical barcodes through repetitive staining, imaging and signal removal steps (top). Different methods for signal amplification (left) include rolling circle amplification (RCA), sequential probe tiling, sequential steps of hybridization, click chemistry amplification, and branched DNA structures. Readouts (right) include *in situ* sequencing in a targeted or untargeted manner, using sequencing by ligation or sequencing by synthesis; or barcode generation by hybridizing fluorescently labeled probes to each target. These barcodes can be binary, using on-off patterns, colorimetric patterns, or both.

information. Different indexing techniques differ in how barcodes are spatially distributed, using printed spots (e.g., ZipSeq),³¹ beads (e.g., Slide-seq, Drop-seq, HDST [high-definition spatial transcriptomics]),^{32–35} clustered arrays (e.g., ST [spatial transcriptomics], Seq-Scope),^{36–38} microwells (e.g., XYZseq,³⁹ or DNA nanoballs (e.g., Stereo-Seq).⁴⁰

The size and density of the barcode spots determine the separation resolution between gene expression profiles. The molecular capture resolution of these methods ranges from 500 to 0.25 μm. When the capture resolution is larger than a single cell size, in methods such as 10x Visium^{36,37} and Slide-seq,³⁵ specific cell types need to be inferred. Inference is done using spot deconvolution or gene expression signatures integrated

from single-cell RNA sequencing (scRNA-seq).^{39,41,42} Methods with subcellular capture resolution, such as Seq-Scope³⁸ and Stereo-seq,⁴⁰ retain single-cell resolution but face challenges resulting from data sparsity and difficulty in determining cell borders.

Altogether, spatial indexing-based methods are powerful in enabling to probe the entire transcriptome in an unbiased manner, not requiring prior knowledge about which genes to measure. As spatial indexing relies on polyA hybridization, a challenge for these methods is the integrity of mRNA in the tissue, which can vary between fresh-frozen and formalin-fixed paraffin-embedded (FFPE) samples. This is an important consideration for cancer research, as clinical samples are often kept as

FFPE blocks. Furthermore, achieving single-cell resolution remains a technical and computational challenge.

Imaging approaches

Imaging-based approaches use fluorescent tagging of mRNA molecules *in situ* and high-resolution fluorescence microscopy to detect and differentiate between single mRNA transcripts. Multiplexing is enabled by performing cycles of tagging, imaging and signal removal, where the different methods differ in their implementation of these basic steps (Figure 1B). A major challenge for imaging-based approaches is that mRNA abundance *in situ* is low and it is often degraded. Therefore, generating specific, bright and robust fluorescent signals from a small number of molecules requires signal amplification. Thus, another large source of variation between the methods is their solutions for signal amplification.

To amplify the signal from individual mRNA molecules, it is customary to build molecular scaffolds on the target RNA, providing a larger addressable sequence for fluorescent labeling. This can be done using enzymes, hybridization or a combination of the two. For example, *in situ* sequencing approaches use padlock probes that bind either the mRNA or reverse-transcribed cDNA, to create a local amplification of either a synthetic barcode sequence or a part of the gene sequence. Different methods use specific combinations of *in situ* cDNA synthesis,^{43–45} rolling circle amplification (e.g., ISS [*in situ* sequencing], FISSEQ [fluorescent *in situ* sequencing], PLISH [proximity ligation *in situ* hybridization]),^{43–46} RNA-templated DNA ligases (e.g., BOLORAMIS [barcoded oligonucleotides ligated on RNA amplified for multiplexed and parallel *in situ* analyses]),⁴⁷ custom padlock probes (e.g., BaristaSeq [barcode *in situ* targeted sequencing], SCRINSHOT [single-cell-resolution *in situ* hybridization on tissues], ExSeq [expansion sequencing], STARmap [spatially resolved transcript amplicon readout mapping]),^{48–51} and expansion microscopy.⁵⁰ Hybridization-based approaches perform enzyme-free signal amplification by tiling multiple probes on the mRNA (e.g., MERFISH [multiplexed error-robust fluorescence *in situ* hybridization], SeqFISH [sequential fluorescence *in situ* hybridization], split-FISH, osmFISH [ouroboros single-molecule fluorescence *in situ* hybridization], EASI-FISH [expansion-assisted iterative fluorescence *in situ* hybridization]),^{52–56} using pre-synthesized amplification structures like branched DNA (e.g., RNAScope),^{57–59} performing rounds of consecutive hybridization reactions (e.g., HCR [hybridization chain reaction], SABER-FISH [signal amplification by exchange reaction fluorescence *in situ* hybridization])^{60,61} or click chemistry (e.g., ClampFISH [click-amplifying fluorescence *in situ* hybridization]).⁶²

After amplification, the mRNAs are decoded using consecutive rounds of imaging. Here too, methods differ but can be broadly grouped into two classes. The first class performs optical-based sequencing of either the barcode or the amplified mRNA sequence using sequencing by synthesis or sequencing by ligation.^{43,45,47,48} The result is a DNA sequence that can be mapped back to a specific mRNA. Although in most approaches this is a synthetic barcode sequence, in some approaches the sequence is derived from the mRNA itself, making it possible to identify splice variants, mutations, SNPs, etc.^{44,47,50,51,63} The second class uses fluorescently labeled probes that

hybridize with the amplified mRNA. The result is fluorescent on-and-off patterns that, in turn, represent barcodes of individual mRNAs.^{52,53,64}

SPATIAL MULTIPLEXED PROTEOMICS

In situ proteomics can be divided to non-targeted approaches, reviewed elsewhere,^{65–68} and targeted approaches using antibodies. For the purpose of this review, we focus on the latter. Most technologies for targeted multiplexed proteomics perform antibody staining using experimental procedures that are similar to those developed for microscopy. Methods differ in the nature of the moieties that are attached to the antibodies, including fluorophores, enzymes, DNA oligos, and metal isotopes. In general, they can be divided into microscopy-based methods and mass spectrometry-based methods.

Cyclic microscopy methods

Light microscopy and fluorescent microscopy make it possible to detect only a handful of targets simultaneously because of spectral overlap. To increase the number of targets imaged, cyclic microscopy methods perform a variation of a cyclic process that involves several steps: (1) tissue staining using tagged antibodies, (2) image acquisition, and (3) signal inactivation or removal (Figure 2A). Iterating over this basic sequence makes it possible to increase the number of proteins imaged but has several challenges. First, the process is time consuming, which can hinder throughput. Second, tissue and epitope integrity may drop across cycles. Third, signal from one cycle can carry over to another because of incomplete removal. Different methods differ in how they address these challenges by modifying both the staining and removal stages.

Multiplexed immunohistochemistry (mIHC) involves sequential rounds of chromogenic staining and imaging followed by signal wash and antibody stripping.⁶⁹ In this method, one antibody is imaged in every cycle, and its application was demonstrated for staining with 12 different antibodies.⁷⁰ Multiplexed immunofluorescence methods make it possible to stain with several antibodies labeled with different fluorophores in every cycle, thus increasing the number of proteins imaged per cycle, reaching dozens of proteins altogether. These methods mostly use primary fluorophore-tagged antibodies, and they differ in the way the fluorophore signal is removed, on the basis of chemical removal (MxIF [multiplexed fluorescence microscopy],⁷¹ IBEX [iterative bleaching extends multiplexity]⁷²) photo-bleaching (MELC [multi-epitope ligand cartography]⁷³), their combination (t-CyCIF [tissue-based cyclic immunofluorescence]⁷⁴), or engineered antibodies that facilitate label release (MICS [MACSima imaging cyclic staining]⁷⁵). To amplify the signal, it is possible to use fluorophore-tagged secondary antibodies that bind to the primary antibodies (4i⁷⁶). Coupling the microscope to automated microfluidics systems that perform the staining and removal stages, reduces hands-on time and improves tissue integrity.^{72,75,77}

To reduce the time associated with multiplexed imaging, different approaches unite either the cyclic staining or imaging into one-step. For example, several approaches use primary antibodies labeled with unique DNA oligos. This makes it possible to perform the lengthy process of antibody hybridization only

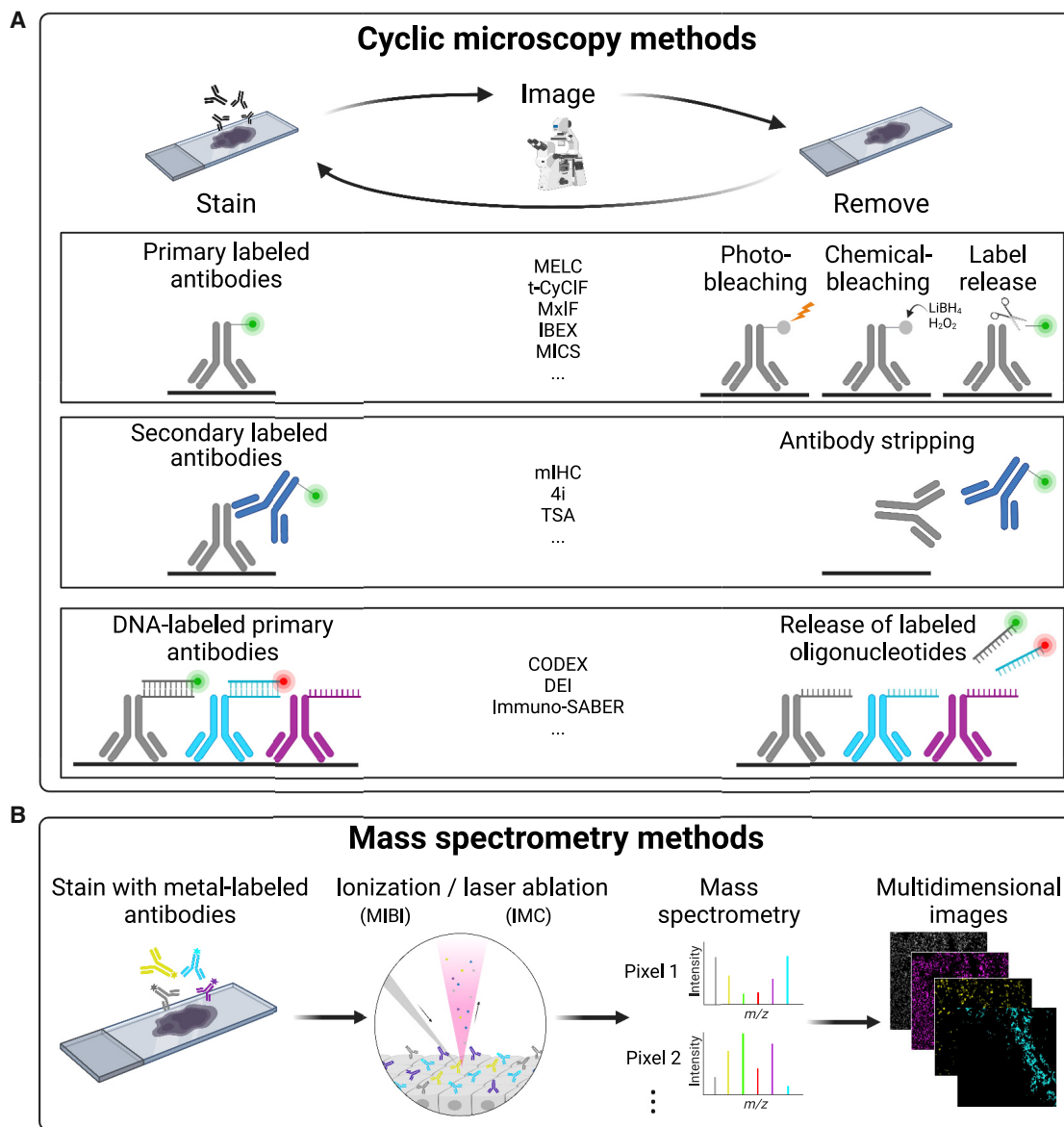


Figure 2. Technologies for targeted spatial profiling of proteins

Multiplexed imaging technologies are divided into cyclic microscopy methods and mass spectrometry-based methods.

(A) Cyclic microscopy performs an iterative process of staining, imaging and signal removal (top). Methods differ in staining (left) and signal removal (right) stages. (B) Mass spectrometry-based methods involve a single staining stage with metal-labeled antibodies, followed by pixel-wise tissue ablation and detection of metal isotopes by mass spectrometry. The mass spectra of all pixels is processed to generate multidimensional images.

once and then perform shorter cycles of labeling, imaging and signal removal using fluorescent oligonucleotide probes or polymerization with fluorescent deoxynucleoside triphosphates (dNTPs) (e.g., DEI [DNA exchange imaging]⁷⁸ and CODEX [co-detection by indexing]^{79,80}). The signal of DNA-labeled antibodies can also be amplified using sequential hybridization reactions (e.g., Immuno-SABER).^{81,82} Another method that allows signal amplification with reduced protocol length is tyramide signal amplification (TSA). In each cycle, covalent binding of multiple tyramide-linked fluorophore molecules to the tissue results in a stable amplified signal that enables antibody stripping. Combining TSA with spectrally separated fluorophores, allows

the detection of up to 8 targets in a single image acquisition stage after all staining cycles are completed.⁸³

Mass spectrometry methods

This group of methods use antibodies attached to unique metal isotopes, which can be differentiated using mass spectrometry. Antibodies are labeled with metal tags and are then applied to stain the tissue in a single reaction. To obtain spatial information, the tissue is then divided into a dense grid, and the expression of all targeted proteins is read for each pixel using mass spectrometry (Figure 2B). Approaches differ in how metals are extracted from the tissue, using either secondary ionization (MIBI

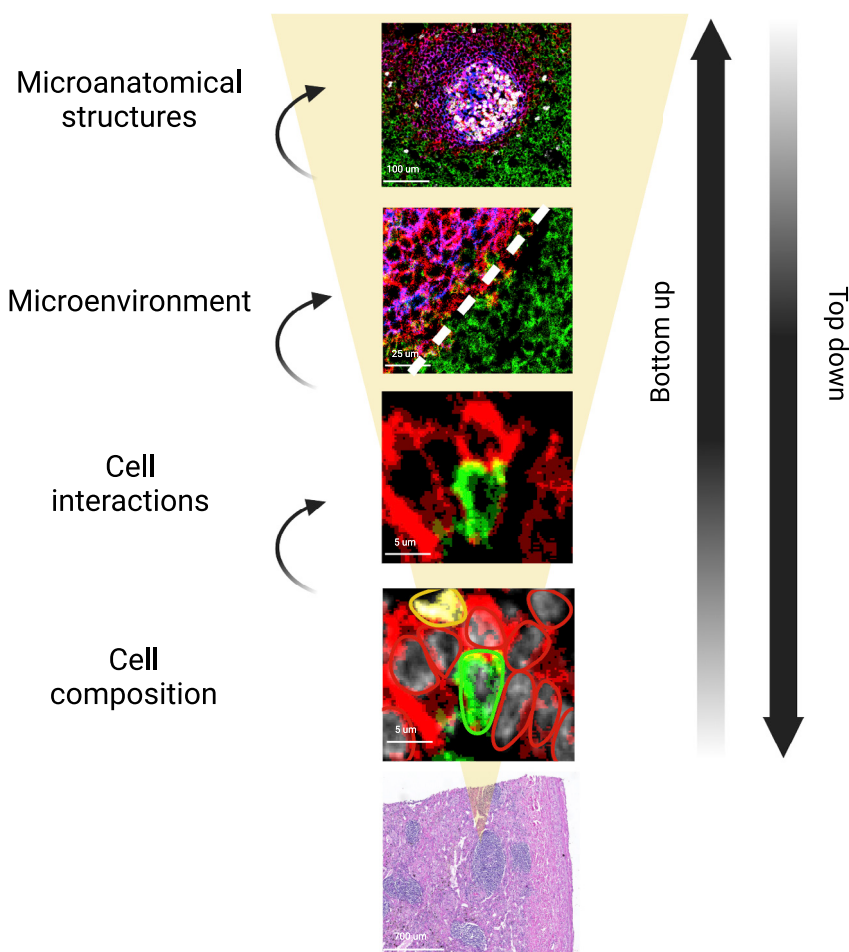


Figure 3. Information scales in spatial profiling

Spatial profiling experiments generate data across length scales, from subcellular to microanatomical structures. Each layer can be used to inform the next, using either bottom-up or top-down analysis methods.

ning tens of thousands of images. This ensemble of images contains multiple layers of information including single-cell phenotypes, single-cell morphology, the composition of cells in the tissue, their close-range interactions, their organization into multi-cellular structures, and the formation of anatomical structures (Figure 3). However, extracting these features from the raw data is not straightforward, and requires dedicated analysis methods, bridging the worlds of microscopy, pathology, single-cell analysis and computer science. In this section, we review the types of information that are derived from spatial profiling technologies, briefly discuss the analytical methods to extract findings from that information, and how these have been used to address questions in cancer.

Single-cell analysis and cell composition

Spatial profiling data contains information regarding the identity and phenotype of

[multiplexed ion beam imaging], MIBI-TOF [time of flight], HD-MIBI [high-definition MIBI],^{84–86} or laser ablation (IMC [imaging mass cytometry]⁸⁷), and in the mass spectrometer, including magnetic sector (MIBI, HD-MIBI) or time of flight (MIBI-TOF, IMC). Unlike microscopy-based methods, these methods are destructive to the tissue.

Altogether, a wide range of technologies is now available for spatial profiling of tissues, and the field is rapidly evolving with novel and improved technologies constantly emerging. Different methodologies differ in their plexing capabilities, simplicity, resolution, cost, ability to detect low-abundance signals, compatibility with clinical specimens and hands-on as well as instrument time. These capabilities should be considered and choice of technology should be adapted to the research questions addressed, available instrumentation, and expertise. In the final two sections of the review, we further discuss these considerations and the specific challenges associated with applying these technologies to cancer research.

SPATIAL PROFILING TECHNOLOGIES IN CANCER RESEARCH

The output of spatial profiling technologies is multidimensional images depicting the spatial expression pattern of each protein or RNA transcript. As such, these present huge datasets, often span-

single cells in the tissue. Although cell composition can be quantified on the basis of single-cell-resolution data, spatial profiling offers several advantages in quantifying cell composition, even when ignoring the spatial aspects. First, depending on technology, one can analyze archived FFPE tissues, whereas suspension-based technologies often require fresh tissue. This allows researchers to infer cellular composition for archived specimens, increasing the number of specimens with long-term clinical follow-up that can be profiled. Second, imaging does not require tissue digestion, which can incur differential loss of specific cell types that are differentially sensitive to digestive conditions (e.g., granulocytes).⁸⁸ Third, imaging makes it possible to characterize extra-cellular components as well as necrotic and fibrotic regions. Altogether, spatial profiling technologies will likely accelerate large-scale and systematic evaluation of cell composition in cancer.

To extract cellular composition from images of spatial profiling, several analytical steps are performed (Figure 4). In methods that offer single-cell resolution, cells are first segmented on the basis of nuclear, cytoplasmic, or membrane stains. Novel segmentation methods mostly rely on human-curated training data to predict cell borders, using supervised machine learning.^{89–93} Following segmentation, the expression of each mRNA or protein is assigned to each cell, generating an *expression matrix*, similar to that obtained from single cell

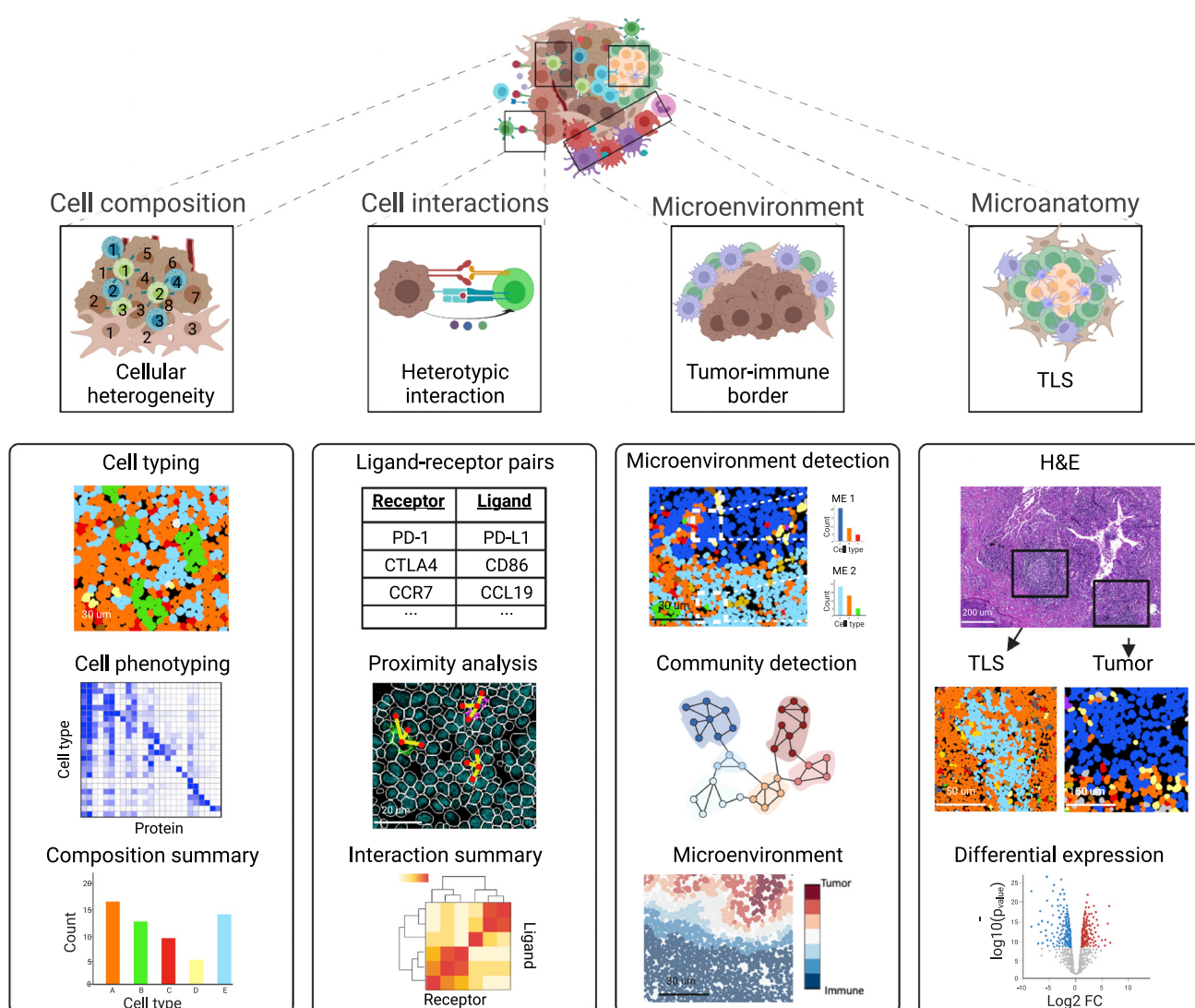


Figure 4. Spatial profiling in cancer research

Exemplary information extracted from spatial profiling technologies in cancer (top). **Cell composition** informs on heterogeneity within the TME. Cells are phenotyped according to the mRNAs or proteins that they express, and the fraction of cells of different types is quantified. **Cell interactions** can be established by examining the proximity between known ligand-receptor pairs. **Microenvironments**, such as the tumor-immune border, can be identified by clustering cells on the basis of the cellular composition of their neighbors or by applying community detection algorithms to detect structural organization within the TME. **Microanatomical structures** such as tertiary lymphoid structures (TLSs) can be identified using histological information, in a top-down approach, and analyzed for differential expression compared with adjacent tissue.

profiling modalities, such as flow cytometry, mass cytometry or scRNA-seq. Next, cells are classified into cell types using clustering and classification algorithms^{94–97} or by a manual sequential gating strategy, similar to analysis of flow cytometry.⁷⁰ The latter is often used to identify rare subtypes of cells.^{75,98,99} In methodologies that do not provide single-cell resolution, such as some of the spatial indexing transcriptomic methods, cellular composition is inferred by deconvolving the gene expression profiles for each spot. Deconvolution models often require expression profiles for each cell type, which can be obtained from scRNA-seq data of the same or similar tissue.^{42,100} Methods differ in the algorithmic implementation of the deconvolution, using non-negative matrix factorization^{35,41} probability,^{101,102} graphs,¹⁰³ and deep learning.^{104,105}

Observations in cancer research

Analysis of cell compositions in solid tumors by spatial profiling highlighted their complexity, including tumor, immune and stromal cell subtypes. Many of these studies focused on characterizing the immune microenvironment. Typically, macrophages and CD8⁺ cytotoxic and CD4⁺ helper T cells are the most abundant immune cells found in various cancer types, whereas other T cells, natural killer (NK) cells, B cells, and granulocytes are found in lower quantities.^{99,106,107} However, across patients, immune infiltration is highly variable, ranging from immune-cold tumors with few or no immune cells to strongly infiltrated tumors.^{98,108} Consistently, various tumors, including head and neck squamous cell carcinoma and pancreatic ductal adenocarcinoma (PDAC) divide into three groups on the basis of leukocyte

profiles: myeloid enriched, lymphoid enriched, and hypo-inflamed.^{70,109}

Mapping cell type composition in multiple tumors makes it possible to examine their co-occurrence within the TME.^{106,110} Interestingly, this approach revealed a similar hierarchical ordering of immune cell composition in several cancers, including melanoma and triple-negative breast cancer. Presence of B cells in the TME is almost always accompanied by helper and cytotoxic T cells, but not vice versa. Similarly, the presence of T cell subtypes is accompanied by macrophages or monocytes.^{108,111} This suggests a coordinated immune response to tumors and may reflect hierarchical recruitment of immune cells to the tumor site.

The cellular composition of tumors is also defined by the phenotypes or states of the cells constituting them. Although cell type composition is typically characterized by the expression of lineage genes, cellular states are defined by co-expression patterns of functional genes. For example, in breast cancer, tumor cell phenotypes characterized by the expression of cytokeratins, hormone receptors, and growth factor receptors reflected clinical subtype.¹¹² A shift in fibroblast subtypes, from resting to cancer-associated fibroblast, associated with transition from ductal carcinoma *in situ* to invasive breast cancer.¹¹³ Functional states of T cells and macrophages have been defined based on co-expression patterns of activation and inhibition molecules and associated with pro- and anti-tumor immune responses.^{70,108,110} For example, clear cell renal cell carcinoma exhibited multiple T cell subtypes defined by combinatorial expression of PD-1, CTLA-4, TIM-3, and ICOS. Furthermore, in these tumors, macrophage populations showed a continuum of phenotypes, of which the CD38⁺CD204⁺CD206⁻ subset associated with an immunosuppressive environment.¹⁰⁶ Taken together, profiling of cellular composition provides information on which cells are present in the tumor microenvironment and their phenotypes and co-occurrences.

Cellular interactions and microenvironmental niches

In addition to information on the composition of cell types and states, spatial profiling technologies include information on their physical location. This makes it possible to map multi-cellular structures in the tissue and provide context for single-cell expression phenotypes. A challenge and opportunity in spatial analyses is that spatial organization spans various connected length scales, including direct interactions, close-range interactions between cells inhabiting a shared microenvironmental niche, and up to organization into microanatomical structures (Figure 3).

To infer various layers of spatial organization, analysis is carried out by either a *top-down* or a *bottom-up* approach. Top-down approaches focus on specific anatomical structures, such as leading edge, tumor core and boundary, on the basis of prior knowledge or histology. Then, unique characteristics of these distinct regions are identified, including gene expression, cellular composition, interactions, etc.^{109,114} In bottom-up approaches, recurrent short-range patterns within the tissue are identified to infer high-order tissue structure. These methods are divided into those that assess pairwise interactions and those that assess multi-

cellular interactions (Figure 4). Pairwise interactions are gauged by identifying pairs of cells,^{98,115} mRNAs¹¹⁶ or proteins,^{117,118} which significantly colocalize in the tissue. One challenge in such analyses is to identify which of these interactions is significant, and to decouple them from interactions resulting from two cell types inhabiting the same microanatomical structure. Limiting the analysis to pre-defined cell types,¹¹¹ histological structures, or known ligand-receptor pairs,^{119,120} can enrich for direct interactions.

Analysis of multi-cellular interactions reveals complex patterns, which may involve more than two cell types. These enrichment patterns are referred to in the literature as cellular neighborhoods, niches, communities, microenvironments, or compartments. Common approaches to identify microenvironmental niches include clustering regions by their cell composition^{99,121,122} and applying community detection algorithms to cellular connectivity graphs^{112,123} (Figure 4). Alternatively, one can directly cluster spatially defined gene expression profiles or gene modules.^{30,42,116,124,125} Altogether, applying spatial methods to large tissue sections makes it possible to identify new regions characterized by multi-cellular interactions, which might not be identified using histological or pathological information and often with higher detail.¹²⁶

Observations in cancer research

Close range. Analysis of close-range interactions in cancer using spatial profiling technologies has revealed general principles of cellular organization. Cellular interactions are grossly divided into homotypic (of the same cell type and phenotype) and heterotypic (of different cell types and phenotypes) interactions. Enrichment in homotypic interactions is a recurrent observation in different cancer types.^{99,108,112} For example, associating cellular interactions with breast cancer subtypes, revealed enriched epithelial and stromal homotypic interactions in basal-like tumors, reflecting separation between these compartments.¹²⁷ These findings emphasize spatial patterning in tumors, which may point to biological activities localized to microenvironmental niches. Supporting this, Hartmann et al.¹²⁸ observed spatial enrichment of proteins from the same metabolic pathways in colorectal tumors, demonstrating niches with distinct localized metabolic activity.

Heterotypic interactions were also described in the TME. Specifically, several studies identified the existence of immune-suppressive microenvironments characterized by interactions of several cellular populations, most predominantly T cells and macrophages. For example, a proliferative suppressive microenvironmental niche in breast cancer showed enrichment of regulatory T cells with lymphocytes expressing immune checkpoint proteins such as PD-1, and macrophages.¹²³ Similarly, a group of high-risk colorectal cancer patients exhibited an enriched suppressive niche of proliferating regulatory T cells and macrophages.⁹⁹ Additional studies identified heterotypic interactions between immunosuppressive macrophages expressing MRC1 and CCL18 and tumor cells in colorectal cancer liver metastasis,¹²⁹ or PD-L1 and IDO1 expressing myeloid cells and tumor cells in breast cancer.⁸⁶

Additional studies identified heterotypic interactions formed by unique populations of tumor cells. For example, in squamous cell carcinoma, a specific tumor cell population that exhibits an invasive gene expression signature, was identified as an

intercellular communication hub on the basis of extensive autocrine and paracrine interactions that they formed with fibroblasts, endothelial cells, macrophages and myeloid-derived suppressor cells.¹³⁰ Similarly, in PDAC a specific subpopulation of cancer cells that expresses stress-response genes colocalized with inflammatory fibroblasts expressing IL-6, while other cancer cell populations did not.⁴² These studies demonstrate an interdependency between localized cellular communication networks and tumor cell phenotypes.

Large scale. Large-scale cellular organizations within the TME appear as distinct spatially defined compartments and microanatomical structures, which can exhibit enrichment in specific cell types. Tumors often organize into a tumor compartment, composed predominantly of tumor cells, and a stromal compartment, consisting mainly of immune cells, fibroblasts, and extracellular matrix (ECM). Indeed, PDAC tumors show enrichment of lymphocytes and myeloid cells in the stromal compartment and immune exclusion from the tumor compartment.^{98,109} In triple-negative breast cancer (TNBC), two subtypes of tissue organization patterns were identified: whereas some tumors exhibit compartmentalization between tumor and immune cells, others demonstrate mixed organization of these cell types.¹¹¹

The interface between compartments in the TME defines borders, or leading edges, which were consistently shown to harbor specific cells, different than those that reside within the compartments. For example, a study comparing cutaneous squamous cell carcinoma and matched normal skin identified a tumor-specific keratinocyte population unique to cancer, localized to a fibro-vascular niche at the tumor leading edge. These cells exhibited gene expression signatures linked to cellular movement, ECM disassembly, and epithelial-to-mesenchymal transition (EMT), consistent with an invasive phenotype.¹³⁰ Similarly, breast cancer tumors show enrichment of myofibroblasts at the tumor-stroma border and depletion of lymphoid cells.¹²³ In TNBC, the tumor-immune border was identified as a site of immune inhibition by PD-L1 expressing myeloid cells and enriched expression of MHCII on tumor cells.^{86,111} These suggest that fibroblasts and macrophages may be essential in supporting the tumor boundary.

Tertiary lymphoid structures (TLSs) present a microanatomical structure that has been identified within a wide range of cancer types. Their structure resembles that of lymphoid follicles with a B cell-rich inner zone surrounded by T cells and populated by additional cell types such as distinct dendritic cell populations, macrophages and fibroblasts.^{131,132} TLSs are considered sites for generating or boosting adaptive immune responses and lymphocyte recruitment. Applying highly multiplexed spatial methodologies to TLSs allows deep characterization of their composition and role in anti-tumor immunity. For example, Meylan et al.¹³³ identified that IgG- and IgA-producing plasma cells spread through a fibroblastic track within TLS-positive tumors in renal cell carcinoma (RCC). Hoch et al.¹³⁴ investigated the spatial distributions of chemokine expression in melanoma and found TLS-dependent gradients of CXCL13, which is involved in B cell follicle maturation. Additionally, this study identified enrichment of TCF1⁺CD8⁺ naïve T cells within TLSs, suggesting that TLSs may serve as the priming site for this subset of cells that is important for anti-tumor immunity.¹³⁵

PROVIDING CONTEXT: ASSOCIATING SPATIAL ORGANIZATION PATTERNS TO TUMOR BIOLOGY, GENETICS, AND CLINICAL PROPERTIES

While the spatial description of the TME is in itself valuable and informative, the next step is to uncover the mechanisms that lead to the formation of these organizational patterns, as well as to reveal their function and clinical implications. To answer these questions, it is necessary to integrate spatial profiling technologies with carefully annotated patient cohorts, additional data and well-controlled perturbations.

Several studies have shown that intrinsic genetic differences between tumors are correlated with the composition and organization of the TME. Work in breast cancer, associated both genetic subtypes of breast cancer and specific genomic alterations with distinct microenvironmental niches.^{136–138} For example, luminal A tumors were depleted of an immune-suppressive niche, which was most enriched in estrogen receptor (ER)-negative tumors. BRCA1 and Casp8 mutations were also associated with an immune-suppressive niche; whereas loss of B2M was associated with TLSs, and gains of CD274 (PD-L1) were associated with a granulocyte-enriched niche.¹²³ These associations reveal a tight connection between tumor genetics and the TME, co-shaping each other.

Murine models, which provide tools to manipulate distinct components in the TME, can provide mechanistic insight and ascertain causal relationships in how tumor cells and other cell types in the TME communicate. This is highlighted in a recent study identifying recurrent cancer cell states across 15 cancer types. By combining scRNA-seq with spatial transcriptomics, they identified co-localization of an interferon-response state in tumor cells with T cells and macrophages. However, in mice lacking lymphocytes, the interferon response module was diminished, whereas the remaining states were unchanged.¹³⁹ Other studies manipulated mutations in cancer cell lines or xenografts before inoculating them into mice, and found that driver mutations, such as PTEN deficiency can influence the growth of other cells in the TME.^{140,141} Integrating murine models with spatial profiling technologies also makes it possible to study the effects of treatment on cellular interactions and cellular composition within distinct tumor compartments.¹⁴² For example, KRAS inhibition in murine orthotopic lung cancer resulted in an expansion of a F4/80⁺CD206⁺MHC-II^{high}CD86^{high} macrophage subtype, which interacts with dendritic cells and fibroblasts. Furthermore, treatment resulted in T cell migration into the tumor domain and improved tumor vascularization.¹⁴³ These results demonstrate how drugs which are thought to have predominantly cell-autonomous effects, such as inhibition of mutated KRAS, also alter the immune response, for example by bringing T cells, macrophages, and tumor cells together to the same compartment.

In addition to murine models, tumor explants are another valuable tool used to study treatment effects on the spatial organization of tumors. Combining targeted secretome analysis with multiplexed imaging on glioblastoma explants treated with anti-CD47 and/or anti-PD-1, identified a subset of explants that induced IFN-γ. These explants, which may represent “responders”, exhibited increased CD4⁺ and CD8⁺ T cells, IFN-γ responses and spatial immune cell rearrangements in the tumor center, but not in the periphery.¹⁴⁴

Finally, applying spatial profiling technologies to large cohorts with annotated clinical information allows associating the TME with progression, survival, and response to treatment. In many cases, these associations were superior upon the integration of spatial information as compared with those obtained from cell type frequencies alone, emphasizing the significance and clinical implications of spatial characterization of tumors.^{99,107,110,112,113,145} Further supporting this, in a meta-analysis conducted to compare predictors to clinical response to anti-PD-1/PD-L1 therapy, multiplexed immunohistochemistry and immunofluorescence had higher diagnostic accuracy than conventional PD-L1 IHC, tumor mutational burden, or bulk gene expression profiling.¹⁴⁶ In another example, Risom et al.¹¹³ used features extracted from multiplexed imaging to train a machine learning model to predict the progression from ductal carcinoma *in situ* to invasive breast cancer. Training on features such as cell type and state, tissue compartment enrichment, cell-cell proximity, and morphometrics, they found that 15 of the top 20 parameters predictive for progression were spatial metrics. Taken together, these findings emphasize the significance of spatial features in patient prognosis.

Specific interactions between cells in the TME were also found to be predictive of prognosis or response to treatment in various cancer types. In high-grade serous ovarian carcinoma, Zhu et al.¹¹⁰ identified 120 nearest neighbor cell-cell interactions that associated with survival, including interactions of granzyme B⁺ cytotoxic T cells and multiple tumor cell subtypes. SpatialScore, which calculates the ratio of distances between CD4⁺ T cells and tumor cells and CD4⁺ T cells and T regulatory cells, was associated with response to anti-PD-1 therapy in cutaneous T cell lymphomas.¹⁰⁷ Additional studies in several cancer types demonstrated associations between distances of immune cell subtypes to tumor cells and patient outcomes.^{98,108,147} Further evidence of the importance of an organized immune response against tumors comes from the association of TLSs with patient outcomes and response to immunotherapy in multiple cancer types.^{131,148–152} In breast cancer, four types of micro-environmental niches were described to associate with survival, with a niche characterized by cellular proliferation and regulatory and dysfunctional T cells associated with the worst prognosis.¹²³ Additional studies demonstrated similar associations between niche organization and patient survival in breast and colorectal cancer.^{99,112,121}

Altogether, these associations to clinical outcomes emphasize that spatial features and organizational patterns within the TME hold valuable information with important clinical implications that could be used in the future for diagnosis or stratification of patients for tailored therapies.

CHALLENGES IN APPLYING SPATIAL TECHNOLOGIES TO CANCER RESEARCH

The application of spatial profiling to cancer holds promise to unravel the structure and function of the tumor microenvironment, but the field is still in its infancy and needs to overcome several challenges to unlock its full potential. One of the greatest challenges of currently available technologies is limited throughput. Cancer-related studies require large cohort sizes to overcome inter-tumor and intra-tumor heterogeneity and obtain meaningful

results. This is true for experiments in murine models, and is dramatically exacerbated in tumors from human patients, where increased biological and environmental heterogeneity is compounded with variability in patient care, and technical differences in handling of tissue samples. However, as many spatial profiling techniques rely on newly developed technologies, their throughput is still limited relative to the needs of the field.

To date, several factors combine to limit the throughput of spatial profiling. Most often, there are trade-offs between these factors, with each playing a bigger or smaller role, depending on the specific technology. One major factor is the high cost of infrastructure and instrumentation and the high costs of reagents and consumables. As a result, cohort sizes are often compromised in favor of costs. One popular solution to increase cohort sizes while maintaining costs at a reasonable level is to use tissue microarrays, which allow studying a large number of samples in a single tissue block. However, this compromises the area of tissue profiled per sample, and results may be skewed by intra-tumor heterogeneity.¹⁰⁹ As the different technologies mature, we can expect costs to drop. For example, exciting developments in sequencing are offering to reduce costs dramatically, which will have profound implications for sequencing-based spatial profiling.¹⁵³

Another important factor that currently limits the throughput of spatial profiling experiments is time. Time can be divided to the time needed to invest before conducting an experiment, hands-on time during an experiment, instrument time and analysis time. To date, many of the spatial profiling technologies require a substantial investment of time before performing an experiment. For example, it requires time and expertise to design good probes and a robust barcoding scheme for probe-based mRNA profiling. In antibody-based multiplexed imaging approaches, it takes time and effort to validate that an antibody clone is compatible with label-conjugation and the multiplexed staining conditions used. Combining a pool of antibodies into panels is also time consuming, because of interference between imaging cycles in cyclic fluorescence or channels in mass-based approaches.^{154–156} Once an experiment is calibrated, acquiring spatial data also takes time. Hands-on time is especially limiting, and many technologies try to minimize it by using microfluidic devices.^{72,75,77} Long running times for instruments, also restrict throughput. This issue is most relevant to microscopy or mass spectrometry-based approaches, in which imaging time scales linearly with the number of samples and size of scanned area. Moreover, the small size of tissue biopsies and the use of single sections may result in sampling bias and miss important elements of the TME in other tumor areas. Finally, analysis of these multiplexed datasets is complex and time consuming.

In the future, we can expect to see technological, analytical, and procedural developments that will dramatically shorten the time frame of all stages of spatial profiling experiments. Increasing the availability of reagents that are compatible with spatial profiling will give a great boost to the field. For example, although secreted factors such as interleukins and chemokines are of major interest for the characterization of cellular communication networks in cancer, availability of antibodies to detect them *in situ* is often limited. Similarly, detection of phosphorylated or mutated proteins that are highly relevant for cancer research, is also limited by the availability and quality of

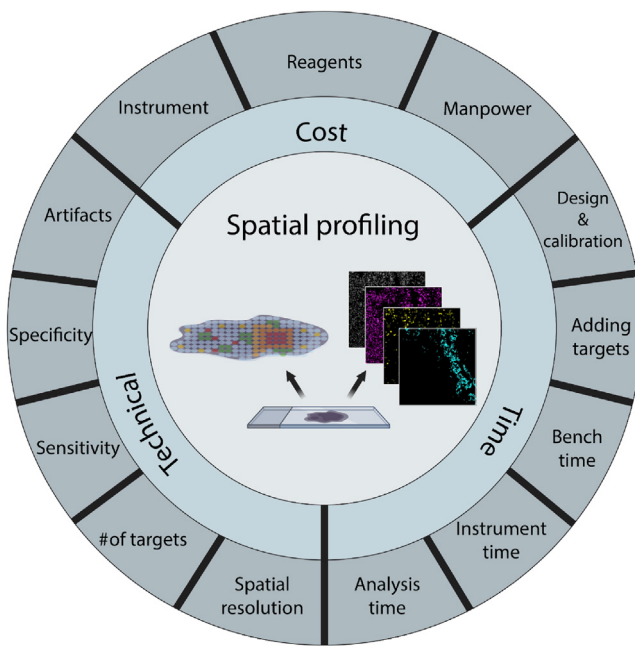


Figure 5. Challenges, considerations, and trade-offs in spatial profiling technologies

antibodies. Standardization of protocols, reagents and analysis pipelines will also be key. Calibration time could be expedited by creating resources for the community that integrate knowledge from different labs and companies regarding antibody clones, hybridization probes, and experimental protocols, as well as commercializing standardized controls for testing them.¹⁵⁷ We can also expect to see more off-the-shelf pre-calibrated antibody panels and mRNA profiling kits.

Importantly, all existing technologies have built-in trade-offs between cost, time and technical performance (Figure 5). Spatial resolution, number of mRNAs or proteins measured, and the quality of the resulting data, including specificity and sensitivity, are also traded one against another across technologies. For example, increasing spatial resolution is possible in most technologies, and is expected to improve the quality of the data, but it currently requires prohibitive increases in imaging time or cost. Similarly, using pre-calibrated reagents can expedite experiments, but often limits the number and variety of molecular targets that are profiled.

As spatial profiling technologies continue to develop, we can expect minimization of these trade-offs: better data for less money and in shorter timescales. Improvements in existing technologies will allow increased resolutions for detailed characterization of subcellular compartments either by physically reducing pixel size^{40,85} or by applying tissue expansion protocols.⁵⁰ In addition, for microscopy and mass spectrometry-based approaches, plexing capabilities are expected to increase by development of new labels¹⁵⁸ and compression/decompression algorithms that make it possible to visualize a larger number of molecules than the number of available labels.¹⁵⁹ Three-dimensional profiling of tissues will provide a more accurate view of the tumor microenvironment as some tissue organization patterns may not be detectable in two di-

mensions. Several studies have already demonstrated multiplexed three-dimensional characterization of mRNA by harnessing hydrogel-tissue chemistry⁵¹ or protein using tissue clearing,¹⁶⁰ serial sectioning of tissues,¹⁶¹ or increasing resolution in ion beam imaging.⁸⁵

FUTURE PERSPECTIVE ON SPATIAL PROFILING IN CANCER RESEARCH

The field of spatial profiling is rapidly evolving, and compelling developments are forthcoming, including consolidation of data modalities, integration with the clinic and large-scale community-based efforts for data sharing. One of the most exciting avenues stems from the possibility to integrate spatial profiling with another technological revolution, the rapidly advancing fields of computer vision and artificial intelligence. The field of computer vision has seen unprecedented developments in the last decade with the introduction of deep learning-based algorithms, which can process images to identify individual people, interpret their facial expressions, and drive cars.^{162–164} Similar algorithms are increasingly being used for a variety of tasks in biological and medical image analysis, from radiology to electron microscopy.^{165,166} Applying computer vision algorithms to tissues stained with H&E already demonstrated automatically learned spatial and morphological features that associate with prognosis and genetic aberrations,¹⁶⁷ highlighting its potential application to analyze multiplexed spatial data. Spatial profiling technologies generate vast datasets, which are very difficult to process manually. Deep learning requires large amounts of data to train. Integrating the two has potential to lead to novel discoveries, which could translate to clinical biomarkers and therapeutics. Already, deep learning has accelerated specific stages in the analysis process, such as cell segmentation and classification.^{93,168} As spatial profiling datasets accumulate, we can expect to see deep learning taking a center-stage role in analysis.

To integrate spatial profiling with deep learning-enabled computer vision, it will be necessary to build standardized infrastructures for data analysis, storage, integration, and sharing. Spatial profiling technologies output large multidimensional files and their large size limits data sharing. Standardization of data generation and file formats through automated and consistent processing pipelines, as well as dedicated web servers for storage and browsing will be critical to drive both computational innovations and biological insights.^{169,170} As part of this effort to standardize and share data, we can expect spatial profiling technologies to play a major role in large-scale community efforts to map tissues in health and disease, including the Human Cell Atlas, the Human BioMolecular Atlas Program and the Human Tumor Atlas Network.^{171–173}

As the field evolves, we can expect technological advancements that will make it possible to map tissues with greater detail. New developments will allow analyzing the spatial distribution of a wide range of molecular components from all omics fields. These include the epigenome, epitranscriptome, secretome, T cell receptor repertoire, microbiome, etc. Novel technologies have already begun to characterize chromatin architecture,^{7,8} accessibility,¹⁷⁴ histone modifications,¹⁷⁵ and translatome.¹⁷⁶

Although spatial mapping of either of the molecular components described in this review, yields valuable findings, integration of these technologies in the same study can connect these layers of information to lend insight into mechanism and function. For example, spatial characterization of the genome in combination with gene expression can provide insights into the influence of genotype on phenotype and decouple genetic and microenvironmental effects in cancer.¹⁰ Integration of modalities can either be done in serial or in a single tissue section. The latter requires development of protocols suitable for characterization of more than one type of molecular component. This is challenging because modalities differ in tissue processing conditions. Nonetheless, protocols for multiplexed characterization of mRNA transcripts and proteins were published,^{59,134,177} and we expect additional developments of integrative protocols in the future.

Beyond integration of technologies, as spatial profiling technologies chart the tumor microenvironment with increasing level of detail, a key next step will be to set up experimental systems that make it possible to functionally interrogate these cellular ecosystems. Analogous to experiments where a particular gene is knocked out or over-expressed to assess its functional role in a process, we need experimental systems that will allow accurate control of the composition, state and organization of individual cells in the tumor. Methods for controlled cell assembly *in vitro*, such as organoid systems or synthetically programmed cell interactions, may provide a framework for such experimental systems.^{178,179} Notably, it is somewhat unclear what would be the relevant perturbations to such a system. Do we entirely remove a cell type? Do we alter the state of the cell? Or do we introduce a different cell type to the ecosystem? Although we do not yet have answers for these complex questions, approaching the tumor microenvironment as an ecosystem of interacting cells, influencing each other's function, certainly offers exciting opportunities for "next-generation" cancer research.

An important front for harnessing the full potential of spatial profiling technologies into cancer research is collaboration with the clinic. Applying spatial profiling to large cohorts with rich, curated clinical metadata will be vital. To this end, spatial profiling technologies must be compatible with clinical practices and workflows. For example, most spatial transcriptomic methods were first developed for fresh-frozen tissues. However, clinical samples are routinely kept as FFPE tissues. In the future we can expect to see either tighter collaborations that will increase the availability of frozen samples for research or technological improvements to facilitate spatial profiling studies on the basis of FFPE material. For example, decrosslinking of fixed tissues¹⁸⁰ or the use of target-specific probes to capture mRNA,¹³³ will improve spatial transcriptomic analysis of FFPE tissues.

Finally, spatial profiling technologies shed light on cellular interactions and microenvironments in the tumor ecosystem. Already, studies show that these features associate with clinical outcomes of patients. As such, we expect that the near future will see the introduction of new biomarkers for diagnosis and stratification of patients for tailored therapies on the basis of interactions among several proteins/genes. Furthermore, these microenvironmental insights could facilitate the development of relevant combination therapies or bispecific antibodies against interacting proteins.^{2,181} Altogether, we foresee that

spatial profiling technologies will continue to evolve, improving our understanding of the tumor microenvironment and playing a major role in both cancer research and clinical care in the years to come.

ACKNOWLEDGMENTS

We thank Dr. Idan Milo for scientific advice and assistance with preparation of figures. O.E. is supported by the Israel Cancer Research Foundation (ICRF) <https://www.icrfonline.org/grants/>. L.K. is supported by the Enoch foundation research fund, the Abisch-Frenkel Foundation, and grants funded by the Schwartz/Reisman Collaborative Science Program, European Research Council (94811), and the Israel Science Foundation (2481/20, 3830/21) within the Israel Precision Medicine Partnership program.

DECLARATION OF INTERESTS

L.K. is a consultant for NucleAI.

REFERENCES

- Mbeunkui, F., and Johann, D.J. (2009). Cancer and the tumor microenvironment: a review of an essential relationship. *Cancer Chemother. Pharmacol.* 63, 571–582. <https://doi.org/10.1007/S00280-008-0881-9/TABLES/2>.
- Jin, M.Z., and Jin, W.L. (2020). The updated landscape of tumor microenvironment and drug repurposing. *Signal Transduct. Targeted Ther.* 5, 166–216. <https://doi.org/10.1038/s41392-020-00280-x>.
- Mignardi, M., Mezger, A., Qian, X., la Fleur, L., Botling, J., Larsson, C., and Nilsson, M. (2015). Oligonucleotide gap-fill ligation for mutation detection and sequencing *in situ*. *Nucleic Acids Res.* 43, e151. <https://doi.org/10.1093/NAR/GKV772>.
- Nguyen, H.Q., Chatteraj, S., Castillo, D., Nguyen, S.C., Nir, G., Lioutas, A., Hershberg, E.A., Martins, N.M.C., Reginato, P.L., Hannan, M., et al. (2020). 3D mapping and accelerated super-resolution imaging of the human genome using *in situ* sequencing. *Nat. Methods* 17, 822–832. <https://doi.org/10.1038/S41592-020-0890-0>.
- Su, J.H., Zheng, P., Kinrot, S.S., Bintu, B., and Zhuang, X. (2020). Genome-scale imaging of the 3D organization and transcriptional activity of chromatin. *Cell* 182, 1641–1659.e26. <https://doi.org/10.1016/J.CELL.2020.07.032>.
- Nir, G., Farabella, I., Pérez Estrada, C., Ebeling, C.G., Beliveau, B.J., Sasaki, H.M., Lee, S.D., Nguyen, S.C., McCole, R.B., Chatteraj, S., et al. (2018). Walking along chromosomes with super-resolution imaging, contact maps, and integrative modeling. *PLoS Genet.* 14, e1007872. <https://doi.org/10.1371/JOURNAL.PGEN.1007872>.
- Mateo, L.J., Murphy, S.E., Hafner, A., Cinquini, I.S., Walker, C.A., and Boettiger, A.N. (2019). Visualizing DNA folding and RNA in embryos at single-cell resolution. *Nature* 568, 49–54. <https://doi.org/10.1038/s41586-019-1035-4>.
- Cardozo Gizzi, A.M., Cattoni, D.I., Fiche, J.B., Espinola, S.M., Gurgo, J., Messina, O., Houbron, C., Ogiyama, Y., Papadopoulos, G.L., Cavalli, G., et al. (2019). Microscopy-based chromosome conformation capture enables simultaneous visualization of genome organization and transcription in intact organisms. *Mol. Cell* 74, 212–222.e5. <https://doi.org/10.1016/J.MOLCEL.2019.01.011>.
- Payne, A.C., Chiang, Z.D., Reginato, P.L., Mangiameli, S.M., Murray, E.M., Yao, C.C., Markoulaki, S., Earl, A.S., Labade, A.S., Jaenisch, R., et al. (2021). *In situ* genome sequencing resolves DNA sequence and structure in intact biological samples. *Science* 371, eaay3446. <https://doi.org/10.1126/SCIENCE.AAY3446>.
- Zhao, T., Chiang, Z.D., Morrissey, J.W., LaFave, L.M., Murray, E.M., del Priore, I., Meli, K., Lereau, C.A., Nadaf, N.M., Li, J., et al. (2021). Spatial genomics enables multi-modal study of clonal heterogeneity in tissues. *Nature* 601, 85–91. <https://doi.org/10.1038/s41586-021-04217-4>.
- Merritt, C.R., Ong, G.T., Church, S.E., Barker, K., Danaher, P., Geiss, G., Hoang, M., Jung, J., Liang, Y., McKay-Fleisch, J., et al. (2020). Multiplex

- digital spatial profiling of proteins and RNA in fixed tissue. *Nat. Biotechnol.* 38, 586–599. <https://doi.org/10.1038/s41587-020-0472-9>.
12. Geiss, G.K., Bumgarner, R.E., Birditt, B., Dahl, T., Dowidar, N., Dunaway, D.L., Fell, H.P., Ferree, S., George, R.D., Grogan, T., et al. (2008). Direct multiplexed measurement of gene expression with color-coded probe pairs. *Nat. Biotechnol.* 26, 317–325. <https://doi.org/10.1038/NBT1385>.
 13. Chen, J., Suo, S., Tam, P.P., Han, J.D.J., Peng, G., and Jing, N. (2017). Spatial transcriptomic analysis of cryosectioned tissue samples with Geo-seq. *Nat. Protoc.* 12, 566–580. <https://doi.org/10.1038/NPROT.2017.003>.
 14. Nichterwitz, S., Benitez, J.A., Hoogstraaten, R., Deng, Q., and Hedlund, E. (2018). LCM-seq: a method for spatial transcriptomic profiling using laser capture microdissection coupled with PolyA-based RNA sequencing. *Methods Mol. Biol.* 1649, 95–110. https://doi.org/10.1007/978-1-4939-7213-5_6.
 15. Nichterwitz, S., Chen, G., Aguilera Benitez, J., Yilmaz, M., Storvall, H., Cao, M., Sandberg, R., Deng, Q., and Hedlund, E. (2016). Laser capture microscopy coupled with Smart-seq2 for precise spatial transcriptomic profiling. *Nat. Commun.* 7, 12139. <https://doi.org/10.1038/NCOMMS12139>.
 16. Combs, P.A., and Eisen, M.B. (2013). Sequencing mRNA from cryo-sliced Drosophila embryos to determine genome-wide spatial patterns of gene expression. *PLoS One* 8, e71820. <https://doi.org/10.1371/JOURNAL.PONE.0071820>.
 17. Berghmans, E., van Raemdonck, G., Schildermans, K., Willems, H., Boonen, K., Maes, E., Mertens, I., Pauwels, P., and Baggerman, G. (2019). MALDI mass spectrometry imaging linked with top-down proteomics as a tool to study the non-small-cell lung cancer tumor microenvironment. *Methods Protoc.* 2, 44. <https://doi.org/10.3390/MPS2020044>.
 18. Mund, A., Coscia, F., Kriston, A., Hollandi, R., Kovács, F., Brunner, A.D., Migh, E., Schweizer, L., Santos, A., Bzorek, M., et al. (2022). Deep Visual Proteomics defines single-cell identity and heterogeneity. *Nat. Biotechnol.* 40, 1231–1240. <https://doi.org/10.1038/s41587-022-01302-5>.
 19. Veličković, D., Agtuka, B.J., Stopka, S.A., Vertes, A., Koppenaal, D.W., Paša-Tolić, L., Stacey, G., and Anderton, C.R. (2018). Observed metabolic asymmetry within soybean root nodules reflects unexpected complexity in rhizobacteria-legume metabolite exchange. *ISME J.* 12, 2335–2338. <https://doi.org/10.1038/s41396-018-0188-8>.
 20. Dueñas, M.E., Larson, E.A., and Lee, Y.J. (2019). Toward mass spectrometry imaging in the metabolomics scale: increasing metabolic coverage through multiple on-tissue chemical modifications. *Front. Plant Sci.* 10, 860. <https://doi.org/10.3389/FPLS.2019.00860> /BIBTEX.
 21. Paine, M.R.L., Liu, J., Huang, D., Ellis, S.R., Trede, D., Kobarg, J.H., Heeren, R.M.A., Fernández, F.M., and MacDonald, T.J. (2019). Three-dimensional mass spectrometry imaging identifies lipid markers of medulloblastoma metastasis. *Sci. Rep.* 9, 2205. <https://doi.org/10.1038/S41598-018-38257-0>.
 22. Boyaval, F., van Zeijl, R., Dalebout, H., Holst, S., van Pelt, G., Fariña-Sarasqueta, A., Mesker, W., Tollenaar, R., Morreau, H., Wuhrer, M., and Heijls, B. (2021). N-glycomic signature of stage II colorectal cancer and its association with the tumor microenvironment. *Mol. Cell. Proteomics* 20, 100057. <https://doi.org/10.1074/MCP.RA120.002215>.
 23. Moses, L., and Pachter, L. (2022). Museum of spatial transcriptomics. *Nat. Methods* 19, 534–546. <https://doi.org/10.1038/S41592-022-01409-2>.
 24. Close, J.L., Long, B.R., and Zeng, H. (2021). Spatially resolved transcriptomics in neuroscience. *Nat. Methods* 18, 23–25. <https://doi.org/10.1038/S41592-020-01040-Z>.
 25. Zhuang, X. (2021). Spatially resolved single-cell genomics and transcriptomics by imaging. *Nat. Methods* 18, 18–22. <https://doi.org/10.1038/S41592-020-01037-8>.
 26. Moffitt, J.R., Lundberg, E., and Heyn, H. (2022). The emerging landscape of spatial profiling technologies. *Nat. Rev. Genet.* 23, 741–759. <https://doi.org/10.1038/s41576-022-00515-3>.
 27. Taylor, M.J., Lukowski, J.K., and Anderton, C.R. (2021). Spatially resolved mass spectrometry at the single cell: recent innovations in proteomics and metabolomics. *J. Am. Soc. Mass Spectrom.* 32, 872–894. <https://doi.org/10.1021/JASMS.0C00439>.
 28. Ho, Y., Shu, L., and Yang, Y. (2017). Imaging mass spectrometry for metabolites: technical progress, multimodal imaging, and biological interactions. *WIREs Mechanisms. of. Disease.* 9, e1387. <https://doi.org/10.1002/WSBM.1387>.
 29. Hickey, J.W., Neumann, E.K., Radtke, A.J., Camarillo, J.M., Beuschel, R.T., Albanese, A., McDonough, E., Hatler, J., Wiblin, A.E., Fisher, J., et al. (2021). Spatial mapping of protein composition and tissue organization: a primer for multiplexed antibody-based imaging. *Nat. Methods* 19, 284–295. <https://doi.org/10.1038/s41592-021-01316-y>.
 30. Rao, A., Barkley, D., França, G.S., and Yanai, I. (2021). Exploring tissue architecture using spatial transcriptomics. *Nature* 596, 211–220. <https://doi.org/10.1038/s41586-021-03634-9>.
 31. Hu, K.H., Eichorst, J.P., McGinnis, C.S., Patterson, D.M., Chow, E.D., Kersten, K., Jameson, S.C., Gartner, Z.J., Rao, A.A., and Krummel, M.F. (2020). ZipSeq: barcoding for real-time mapping of single cell transcriptomes. *Nat. Methods* 17, 833–843. <https://doi.org/10.1038/S41592-020-0880-2>.
 32. Stickels, R.R., Murray, E., Kumar, P., Li, J., Marshall, J.L., di Bella, D.J., Arliotta, P., Macosko, E.Z., and Chen, F. (2021). Highly sensitive spatial transcriptomics at near-cellular resolution with Slide-seqV2. *Nat. Biotechnol.* 39, 313–319. <https://doi.org/10.1038/S41587-020-0739-1>.
 33. Macosko, E.Z., Basu, A., Satija, R., Nemesh, J., Shekhar, K., Goldman, M., Tirosh, I., Bialas, A.R., Kamitaki, N., Marstersteck, E.M., et al. (2015). Highly parallel genome-wide expression profiling of individual cells using nanoliter droplets. *Cell* 161, 1202–1214. <https://doi.org/10.1016/J.CELL.2015.05.002>.
 34. Vickovic, S., Eraslan, G., Salmén, F., Klughammer, J., Stenbeck, L., Schapiro, D., Äijö, T., Bonneau, R., Bergenstråhlé, L., Navarro, J.F., et al. (2019). High-definition spatial transcriptomics for *in situ* tissue profiling. *Nat. Methods* 16, 987–990. <https://doi.org/10.1038/S41592-019-0548-Y>.
 35. Rodrigues, S.G., Stickels, R.R., Goeva, A., Martin, C.A., Murray, E., Vanderburg, C.R., Welch, J., Chen, L.M., Chen, F., and Macosko, E.Z. (2019). Slide-seq: a scalable technology for measuring genome-wide expression at high spatial resolution. *Science* 363, 1463–1467. <https://doi.org/10.1126/SCIENCE.AAW1219>.
 36. Salmén, F., Ståhl, P.L., Mollbrink, A., Navarro, J.F., Vickovic, S., Frisén, J., and Lundeberg, J. (2018). Barcoded solid-phase RNA capture for Spatial Transcriptomics profiling in mammalian tissue sections. *Nat. Protoc.* 13, 2501–2534. <https://doi.org/10.1038/S41596-018-0045-2>.
 37. Ståhl, P.L., Salmén, F., Vickovic, S., Lundmark, A., Navarro, J.F., Magnusson, J., Giacomello, S., Asp, M., Westholm, J.O., Huss, M., et al. (2016). Visualization and analysis of gene expression in tissue sections by spatial transcriptomics. *Science* 353, 78–82. <https://doi.org/10.1126/SCIENCE.AAF2403>.
 38. Cho, C.S., Xi, J., Si, Y., Park, S.R., Hsu, J.E., Kim, M., Jun, G., Kang, H.M., and Lee, J.H. (2021). Microscopic examination of spatial transcriptome using Seq-Scope. *Cell* 184, 3559–3572.e22. <https://doi.org/10.1016/J.CELL.2021.05.010>.
 39. Lee, Y., Bogdanoff, D., Wang, Y., Hartoularos, G.C., Woo, J.M., Mowery, C.T., Nisonoff, H.M., Lee, D.S., Sun, Y., Lee, J., et al. (2021). XYSeq: spatially resolved single-cell RNA sequencing reveals expression heterogeneity in the tumor microenvironment. *Sci. Adv.* 7, eabg4755. <https://doi.org/10.1126/SCIADV.ABG4755>.
 40. Chen, A., Liao, S., Cheng, M., Ma, K., Wu, L., Lai, Y., Qiu, X., Yang, J., Xu, J., Hao, S., et al. (2022). Spatiotemporal transcriptomic atlas of mouse organogenesis using DNA nanoball-patterned arrays. *Cell* 185, 1777–1792.e21. <https://doi.org/10.1016/J.CELL.2022.04.003>.
 41. Elosua-Bayes, M., Nieto, P., Mereu, E., Gut, I., and Heyn, H. (2021). SPOTlight: seeded NMF regression to deconvolute spatial transcriptomics spots with single-cell transcriptomes. *Nucleic Acids Res.* 49, E50. <https://doi.org/10.1093/NAR/GKAB043>.
 42. Moncada, R., Barkley, D., Wagner, F., Chiodin, M., Devlin, J.C., Baron, M., Hajdu, C.H., Simeone, D.M., and Yanai, I. (2020). Integrating microarray-based spatial transcriptomics and single-cell RNA-seq reveals

- tissue architecture in pancreatic ductal adenocarcinomas. *Nat. Biotechnol.* 38, 333–342. <https://doi.org/10.1038/s41587-019-0392-8>.
43. Ke, R., Mignardi, M., Pacureanu, A., Svedlund, J., Botling, J., Wählby, C., and Nilsson, M. (2013). In situ sequencing for RNA analysis in preserved tissue and cells. *Nat. Methods* 10, 857–860. <https://doi.org/10.1038/nmeth.2563>.
44. Lee, J.H., Daugharty, E.R., Scheiman, J., Kalhor, R., Ferrante, T.C., Terry, R., Turczyk, B.M., Yang, J.L., Lee, H.S., Aach, J., et al. (2015). Fluorescent in situ sequencing (FISSEQ) of RNA for gene expression profiling in intact cells and tissues. *Nat. Protoc.* 10, 442–458. <https://doi.org/10.1038/NPROT.2014.191>.
45. Gyllborg, D., Langseth, C.M., Qian, X., Choi, E., Salas, S.M., Hilscher, M.M., Lein, E.S., and Nilsson, M. (2020). Hybridization-based in situ sequencing (HybIS) for spatially resolved transcriptomics in human and mouse brain tissue. *Nucleic Acids Res.* 48, E112. <https://doi.org/10.1093/NAR/GKA4792>.
46. Nagendran, M., Riordan, D.P., Harbury, P.B., and Desai, T.J. (2018). Automated cell-type classification in intact tissues by single-cell molecular profiling. *Elife* 7, e30510. <https://doi.org/10.7554/ELIFE.30510>.
47. Liu, S., Punthambaker, S., Iyer, E.P.R., Ferrante, T., Goodwin, D., Fürth, D., Pawlowski, A.C., Jindal, K., Tam, J.M., Mifflin, L., et al. (2021). Bar-coded oligonucleotides ligated on RNA amplified for multiplexed and parallel in situ analyses. *Nucleic Acids Res.* 49, e58. <https://doi.org/10.1093/NAR/GKAB120>.
48. Chen, X., Sun, Y.C., Church, G.M., Lee, J.H., and Zador, A.M. (2018). Efficient in situ barcode sequencing using padlock probe-based BaristaSeq. *Nucleic Acids Res.* 46, e22. <https://doi.org/10.1093/NAR/GKX1206>.
49. Sountoulidis, A., Lontos, A., Nguyen, H.P., Firsova, A.B., Fysikopoulos, A., Qian, X., Seeger, W., Sundström, E., Nilsson, M., and Samakovlis, C. (2020). SCRINSHOT enables spatial mapping of cell states in tissue sections with single-cell resolution. *PLoS Biol.* 18, e3000675. <https://doi.org/10.1371/JOURNAL.PBIO.3000675>.
50. Alon, S., Goodwin, D.R., Sinha, A., Wassie, A.T., Chen, F., Daugharty, E.R., Bando, Y., Kajita, A., Xue, A.G., Marrett, K., et al. (2021). Expansion sequencing: spatially precise in situ transcriptomics in intact biological systems. *Science* 371, eaax2656. <https://doi.org/10.1126/SCIENCE.AAX2656>.
51. Wang, X., Allen, W.E., Wright, M.A., Sylwestrak, E.L., Samusik, N., Vesuna, S., Evans, K., Liu, C., Ramakrishnan, C., Liu, J., et al. (2018). Three-dimensional intact-tissue sequencing of single-cell transcriptional states. *Science* 1979, 361. https://doi.org/10.1126/SCIENCE.AAT5691/SUPPL_FILE/AAT5691_WANG_SM_TABLE-S2.XLSX.
52. Lubeck, E., Coskun, A.F., Zhiyentayev, T., Ahmad, M., and Cai, L. (2014). Single-cell in situ RNA profiling by sequential hybridization. *Nat. Methods* 11, 360–361. <https://doi.org/10.1038/NMETH.2892>.
53. Chen, K.H., Boettiger, A.N., Moffitt, J.R., Wang, S., and Zhuang, X. (2015). RNA imaging. Spatially resolved, highly multiplexed RNA profiling in single cells. *Science* 348, aaa6090. <https://doi.org/10.1126/SCIENCE.AAA6090>.
54. Goh, J.J.L., Chou, N., Seow, W.Y., Ha, N., Cheng, C.P.P., Chang, Y.C., Zhao, Z.W., and Chen, K.H. (2020). Highly specific multiplexed RNA imaging in tissues with split-FISH. *Nat. Methods* 17, 689–693. <https://doi.org/10.1038/S41592-020-0858-0>.
55. Wang, Y., Eddison, M., Fleishman, G., Weigert, M., Xu, S., Wang, T., Rokicki, K., Goina, C., Henry, F.E., Lemire, A.L., et al. (2021). EASI-FISH for thick tissue defines lateral hypothalamus spatio-molecular organization. *Cell* 184, 6361–6377.e24. <https://doi.org/10.1016/J.CELL.2021.11.024>.
56. Codeluppi, S., Borm, L.E., Zeisel, A., Ia Manno, G., van Lunteren, J.A., Svensson, C.I., and Linnarsson, S. (2018). Spatial organization of the somatosensory cortex revealed by osmFISH. *Nat. Methods* 15, 932–935. <https://doi.org/10.1038/S41592-018-0175-Z>.
57. Wang, F., Flanagan, J., Su, N., Wang, L.C., Bui, S., Nielson, A., Wu, X., Vo, H.T., Ma, X.J., and Luo, Y. (2012). RNAscope: a novel in situ RNA analysis platform for formalin-fixed, paraffin-embedded tissues. *J. Mol. Diagn.* 14, 22–29. <https://doi.org/10.1016/j.jmoldx.2011.08.002>.
58. Xia, C., Babcock, H.P., Moffitt, J.R., and Zhuang, X. (2019). Multiplexed detection of RNA using MERFISH and branched DNA amplification. *Sci. Rep.* 9, 7721. <https://doi.org/10.1038/S41598-019-43943-8>.
59. Schulz, D., Zanotelli, V.R.T., Fischer, J.R., Schapiro, D., Engler, S., Lun, X.K., Jackson, H.W., and Bodenmiller, B. (2018). Simultaneous multiplexed imaging of mRNA and proteins with subcellular resolution in breast cancer tissue samples by mass cytometry. *Cell Syst.* 6, 25–36.e5. <https://doi.org/10.1016/J.CELS.2017.12.001>.
60. Dirks, R.M., and Pierce, N.A. (2004). Triggered amplification by hybridization chain reaction. *Proc. Natl. Acad. Sci. USA* 101, 15275–15278. <https://doi.org/10.1073/PNAS.0407024101>.
61. Kishi, J.Y., Lapan, S.W., Beliveau, B.J., West, E.R., Zhu, A., Sasaki, H.M., Saka, S.K., Wang, Y., Cepko, C.L., and Yin, P. (2019). SABER amplifies FISH: enhanced multiplexed imaging of RNA and DNA in cells and tissues. *Nat. Methods* 16, 533–544. <https://doi.org/10.1038/S41592-019-0404-0>.
62. Rouhanifard, S.H., Mellis, I.A., Dunagin, M., Bayatpour, S., Jiang, C.L., Dardani, I., Symmons, O., Emerit, B., Torre, E., Cote, A., et al. (2018). ClampFISH detects individual nucleic acid molecules using click chemistry-based amplification. *Nat. Biotechnol.* 37, 84–89. <https://doi.org/10.1038/nbt.4286>.
63. Lee, J.H., Daugharty, E.R., Scheiman, J., Kalhor, R., Yang, J.L., Ferrante, T.C., Terry, R., Jeanty, S.S.F., Li, C., Amamoto, R., et al. (2014). Highly multiplexed subcellular RNA sequencing in situ. *Science* 343, 1360–1363. <https://doi.org/10.1126/science.1250212>.
64. Eng, C.H.L., Lawson, M., Zhu, Q., Dries, R., Koulena, N., Takei, Y., Yun, J., Cronin, C., Karp, C., Yuan, G.C., and Cai, L. (2019). Transcriptome-scale super-resolved imaging in tissues by RNA seqFISH+. *Nature* 568, 235–239. <https://doi.org/10.1038/s41586-019-1049-y>.
65. Lee, P.Y., Yeoh, Y., Omar, N., Pung, Y.F., Lim, L.C., and Low, T.Y. (2021). Molecular tissue profiling by MALDI imaging: recent progress and applications in cancer research. *Crit. Rev. Clin. Lab. Sci.* 58, 513–529. <https://doi.org/10.1080/10408363.2021.1942781>.
66. Goodwin, R.J.A., Takats, Z., and Bunch, J. (2020). A critical and concise review of mass spectrometry applied to imaging in drug discovery. *SLAS Discovery* 25, 963–976. https://doi.org/10.1177/2472555220941843/ASSET/IMAGES/LARGE/10.1177_2472555220941843-FIG2.JPG.
67. Unsihuay, D., Mesa Sanchez, D., and Laskin, J. (2021). Quantitative mass spectrometry imaging of biological systems. *Annu. Rev. Phys. Chem.* 72, 307–329. <https://doi.org/10.1146/ANNUREV-PHYSCHEM-061020-053416>.
68. Buchberger, A.R., DeLaney, K., Johnson, J., and Li, L. (2018). Mass spectrometry imaging: a review of emerging advancements and future insights. *Anal. Chem.* 90, 240–265. https://doi.org/10.1021/ACS.ANALCHEM.7B04733/ASSET/IMAGES/LARGE/AC-2017-04733G_0009.JPG.
69. Glass, G., Papin, J.A., and Mandell, J.W. (2009). SIMPLE: a sequential immunoperoxidase labeling and erasing method. *J. Histochem. Cytochem.* 57, 899–905. <https://doi.org/10.1369/JHC.2009.953612>.
70. Tsujikawa, T., Kumar, S., Borkar, R.N., Azimi, V., Thibault, G., Chang, Y.H., Balter, A., Kawashima, R., Choe, G., Sauer, D., et al. (2017). Quantitative multiplex immunohistochemistry reveals myeloid-inflamed tumor-immune complexity associated with poor prognosis. *Cell Rep.* 19, 203–217. <https://doi.org/10.1016/j.celrep.2017.03.037>.
71. Gerdes, M.J., Sevinsky, C.J., Sood, A., Adak, S., Bello, M.O., Bordwell, A., Can, A., Corwin, A., Dinn, S., Filkins, R.J., et al. (2013). Highly multiplexed single-cell analysis of formalinfixed, paraffin-embedded cancer tissue. *Proc. Natl. Acad. Sci. USA* 110, 11982–11987. https://doi.org/10.1073/PNAS.1300136110/SUPPL_FILE/SD04.XLSX.
72. Radtke, A.J., Kandov, E., Lowekamp, B., Speranza, E., Chu, C.J., Gola, A., Thakur, N., Shih, R., Yao, L., Yaniv, Z.R., et al. (2020). IBEX: a versatile multiplex optical imaging approach for deep phenotyping and spatial analysis of cells in complex tissues. *Proc. Natl. Acad. Sci. USA* 117, 33455–33465. https://doi.org/10.1073/PNAS.2018488117/SUPPL_FILE/PNAS.2018488117.SM09.MP4.
73. Schubert, W., Bonnekoh, B., Pommer, A.J., Philipsen, L., Böckelmann, R., Malykh, Y., Golnick, H., Friedenberger, M., Bode, M., and Dress, A.W.M. (2006). Analyzing proteome topology and function by automated

- multidimensional fluorescence microscopy. *Nat. Biotechnol.* 24, 1270–1278. <https://doi.org/10.1038/NBT1250>.
74. Lin, J.R., Izar, B., Wang, S., Yapp, C., Mei, S., Shah, P.M., Santagata, S., and Sorger, P.K. (2018). Highly multiplexed immunofluorescence imaging of human tissues and tumors using t-CyCLIF and conventional optical microscopes. *Elife* 7, e31657. <https://doi.org/10.7554/ELIFE.31657>.
 75. Kirkhabwala, A., Herbel, C., Parkratz, J., Yushchenko, D.A., Rüberg, S., Praveen, P., Reiß, S., Rodriguez, F.C., Schäfer, D., Kollet, J., et al. (2022). MACSima imaging cyclic staining (MICS) technology reveals combinatorial target pairs for CAR T cell treatment of solid tumors. *Sci. Rep.* 12, 1911–1916. <https://doi.org/10.1038/s41598-022-05841-4>.
 76. Gut, G., Herrmann, M.D., and Pelkmans, L. (2018). Multiplexed protein maps link subcellular organization to cellular states. *Science* 1979, 361. https://doi.org/10.1126/SCIENCE.AAR7042/SUPPL_FILE/AAR7042_TABLE_S4.CSV.
 77. Kennedy-Darling, J., Bhate, S.S., Hickey, J.W., Black, S., Barlow, G.L., Vazquez, G., Venkataraman, V.G., Samusik, N., Goltsev, Y., Schürch, C.M., and Nolan, G.P. (2021). Highly multiplexed tissue imaging using repeated oligonucleotide exchange reaction. *Eur. J. Immunol.* 51, 1262–1277. <https://doi.org/10.1002/EJI.202048891>.
 78. Wang, Y., Woehrstein, J.B., Donoghue, N., Dai, M., Avendaño, M.S., Schackmann, R.C.J., Zoeller, J.J., Wang, S.S.H., Tillberg, P.W., Park, D., et al. (2017). Rapid sequential *in situ* multiplexing with DNA exchange imaging in neuronal cells and tissues. *Nano Lett.* 17, 6131–6139. https://doi.org/10.1021/ACS.NANOLETT.7B02716/SUPPL_FILE/NL7B02716_SI_002.AVI.
 79. Goltsev, Y., Samusik, N., Kennedy-Darling, J., Bhate, S., Hale, M., Vazquez, G., Black, S., and Nolan, G.P. (2018). Deep profiling of mouse splenic architecture with CODEX multiplexed imaging. *Cell* 174, 968–981.e15. <https://doi.org/10.1016/J.CELL.2018.07.010>.
 80. Black, S., Phillips, D., Hickey, J.W., Kennedy-Darling, J., Venkataraman, V.G., Samusik, N., Goltsev, Y., Schürch, C.M., and Nolan, G.P. (2021). CODEX multiplexed tissue imaging with DNA-conjugated antibodies. *Nat. Protoc.* 16, 3802–3835. <https://doi.org/10.1038/s41596-021-00556-8>.
 81. Saka, S.K., Wang, Y., Kishi, J.Y., Zhu, A., Zeng, Y., Xie, W., Kirli, K., Yapp, C., Cicconetti, M., Beliveau, B.J., et al. (2019). Immuno-SABER enables highly multiplexed and amplified protein imaging in tissues. *Nat. Biotechnol.* 37, 1080–1090. <https://doi.org/10.1038/s41587-019-0207-y>.
 82. Lin, R., Feng, Q., Li, P., Zhou, P., Wang, R., Liu, Z., Wang, Z., Qi, X., Tang, N., Shao, F., and Luo, M. (2018). A hybridization-chain-reaction-based method for amplifying immunosignals. *Nat. Methods* 15, 275–278. <https://doi.org/10.1038/nmeth.4611>.
 83. Stack, E.C., Wang, C., Roman, K.A., and Hoyt, C.C. (2014). Multiplexed immunohistochemistry, imaging, and quantitation: a review, with an assessment of Tyramide signal amplification, multispectral imaging and multiplex analysis. *Methods* 70, 46–58. <https://doi.org/10.1016/J.YMETH.2014.08.016>.
 84. Angelo, M., Bendall, S.C., Finck, R., Hale, M.B., Hitzman, C., Borowsky, A.D., Levenson, R.M., Lowe, J.B., Liu, S.D., Zhao, S., et al. (2014). Multiplexed ion beam imaging of human breast tumors. *Nat. Med.* 20, 436–442. <https://doi.org/10.1038/nm.3488>.
 85. Rovira-Clavé, X., Jiang, S., Bai, Y., Zhu, B., Barlow, G., Bhate, S., Coskun, A.F., Han, G., Ho, C.M.K., Hitzman, C., et al. (2021). Subcellular localization of biomolecules and drug distribution by high-definition ion beam imaging. *Nat. Commun.* 12, 4628. <https://doi.org/10.1038/S41467-021-24822-1>.
 86. Keren, L., Bosse, M., Thompson, S., Risom, T., Vijayaraghavan, K., McCaffrey, E., Marquez, D., Angoshtari, R., Greenwald, N.F., Fienberg, H., et al. (2019). MIBI-TOF: a multiplexed imaging platform relates cellular phenotypes and tissue structure. *Sci. Adv.* 5, eaax5851. <https://doi.org/10.1126/sciadv.aax5851>.
 87. Giesen, C., Wang, H.A.O., Schapiro, D., Zivanovic, N., Jacobs, A., Hattendorf, B., Schüffler, P.J., Grönlund, D., Buhmann, J.M., Brandt, S., et al. (2014). Highly multiplexed imaging of tumor tissues with subcellular resolution by mass cytometry. *Nat. Methods* 11, 417–422. <https://doi.org/10.1038/nmeth.2869>.
 88. Qiu, P. (2020). Embracing the dropouts in single-cell RNA-seq analysis. *Nat. Commun.* 11, 1169. <https://doi.org/10.1038/s41467-020-14976-9>.
 89. Stringer, C., Wang, T., Michaelos, M., and Pachitariu, M. (2020). Cellpose: a generalist algorithm for cellular segmentation. *Nat. Methods* 18, 100–106. <https://doi.org/10.1038/s41592-020-01018-x>.
 90. Van Valen, D.A., Kudo, T., Lane, K.M., Macklin, D.N., Quach, N.T., DeFelice, M.M., Maayan, I., Tanouchi, Y., Ashley, E.A., and Covert, M.W. (2016). Deep learning automates the quantitative analysis of individual cells in live-cell imaging experiments. *PLoS Comput. Biol.* 12, e1005177. <https://doi.org/10.1371/journal.pcbi.1005177>.
 91. McQuin, C., Goodman, A., Chernyshev, V., Kamentsky, L., Cimini, B.A., Karhohs, K.W., Doan, M., Ding, L., Rafelski, S.M., Thirstrup, D., et al. (2018). CellProfiler 3.0: next-generation image processing for biology. *PLoS Biol.* 16, e2005970. <https://doi.org/10.1371/JOURNAL.PBIO.2005970>.
 92. Berg, S., Kutra, D., Kroeger, T., Straehle, C.N., Kausler, B.X., Haubold, C., Schiegg, M., Ales, J., Beier, T., Rudy, M., et al. (2019). ilastik: interactive machine learning for (bio)image analysis. *Nat. Methods* 16, 1226–1232. <https://doi.org/10.1038/s41592-019-0582-9>.
 93. Greenwald, N.F., Miller, G., Moen, E., Kong, A., Kagel, A., Dougherty, T., Fullaway, C.C., McIntosh, B.J., Leow, K.X., Schwartz, M.S., et al. (2021). Whole-cell segmentation of tissue images with human-level performance using large-scale data annotation and deep learning. *Nat. Biotechnol.* 40, 555–565. <https://doi.org/10.1038/s41587-021-01094-0>.
 94. Bankhead, P., Loughrey, M.B., Fernández, J.A., Dombrowski, Y., McArt, D.G., Dunne, P.D., McQuaid, S., Gray, R.T., Murray, L.J., Coleman, H.G., et al. (2017). QuPath: open source software for digital pathology image analysis. *Sci. Rep.* 7, 16878–16887. <https://doi.org/10.1038/s41598-017-17204-5>.
 95. Van Gassen, S., Callebaut, B., Van Helden, M.J., Lambrecht, B.N., Demester, P., Dhaene, T., and Saeys, Y. (2015). FlowSOM: using self-organizing maps for visualization and interpretation of cytometry data. *Cytometry A* 87, 636–645. <https://doi.org/10.1002/CYTO.A.22625>.
 96. Levine, J.H., Simonds, E.F., Bendall, S.C., Davis, K.L., Amir, E.A.D., Tadmor, M.D., Litvin, O., Fienberg, H.G., Jager, A., Zunder, E.R., et al. (2015). Data-driven phenotypic dissection of AML reveals progenitor-like cells that correlate with prognosis. *Cell* 162, 184–197. <https://doi.org/10.1016/J.CELL.2015.05.047>.
 97. Stuart, T., Butler, A., Hoffman, P., Hafemeister, C., Papalexi, E., Mauck, W.M., Hao, Y., Stoeckius, M., Smibert, P., and Satija, R. (2019). Comprehensive integration of single-cell data. *Cell* 177, 1888–1902.e21. <https://doi.org/10.1016/J.CELL.2019.05.031>.
 98. Väyrynen, S.A., Zhang, J., Yuan, C., Väyrynen, J.P., Dias Costa, A., Williams, H., Morales-Oyarvide, V., Lau, M.C., Robinson, D.A., Dunne, R.F., et al. (2020). Composition, spatial characteristics, and prognostic significance of myeloid cell infiltration in pancreatic cancer. *Clin. Cancer Res.* 3141, 2020. <https://doi.org/10.1158/1078-0432.ccr-20-3141>.
 99. Schürch, C.M., Bhate, S.S., Barlow, G.L., Phillips, D.J., Noti, L., Zlobec, I., Chu, P., Black, S., Demeter, J., McIlwain, D.R., et al. (2020). Coordinated cellular neighborhoods orchestrate antitumoral immunity at the colorectal cancer invasive. *Cell* 182, 1341–1359.e19. <https://doi.org/10.1016/J.CELL.2020.07.005>.
 100. Hwang, W.L., Jagadeesh, K.A., Guo, J.A., Hoffman, H.I., Yadollahpour, P., Reeves, J.W., Mohan, R., Droklyansky, E., Van Wittenbergh, N., Ashenberg, O., et al. (2022). Single-nucleus and spatial transcriptome profiling of pancreatic cancer identifies multicellular dynamics associated with neoadjuvant treatment. *Nat. Genet.* 54, 1178–1191. <https://doi.org/10.1038/s41588-022-01134-8>.
 101. Cable, D.M., Murray, E., Zou, L.S., Goeva, A., Macosko, E.Z., Chen, F., and Irizarry, R.A. (2021). Robust decomposition of cell type mixtures in spatial transcriptomics. *Nat. Biotechnol.* 40, 517–526. <https://doi.org/10.1038/s41587-021-00830-w>.
 102. Andersson, A., Bergenstråhlé, J., Asp, M., Bergenstråhlé, L., Jurek, A., Fernández Navarro, J., and Lundeberg, J. (2020). Single-cell and spatial transcriptomics enables probabilistic inference of cell type topography. *Commun. Biol.* 3, 565. <https://doi.org/10.1038/S42003-020-01247-Y>.

103. Song, Q., and Su, J. (2021). DSTG: deconvoluting spatial transcriptomics data through graph-based artificial intelligence. *Briefings Bioinf.* 22, bbaa414–13. <https://doi.org/10.1093/BIB/BBA414>.
104. Biancalani, T., Scalia, G., Buffoni, L., Avasthi, R., Lu, Z., Sanger, A., Tokcan, N., Vanderburg, C.R., Segerstolpe, A., Zhang, M., et al. (2021). Deep learning and alignment of spatially resolved single-cell transcriptomes with Tangram. *Nat. Methods* 18, 1352–1362. <https://doi.org/10.1038/s41592-021-01264-7>.
105. Nelson, M.E., Riva, S.G., and Cvejic, A. (2022). SMaSH: a scalable, general marker gene identification framework for single-cell RNA-sequencing. *BMC Bioinf.* 23, 328–416. <https://doi.org/10.1186/S12859-022-04860-2/TABLES/2>.
106. Chevrier, S., Levine, J.H., Zanotelli, V.R.T., Silina, K., Schulz, D., Bacac, M., Ries, C.H., Ailles, L., Jewett, M.A.S., Moch, H., et al. (2017). An immune atlas of clear cell renal cell carcinoma. *Cell* 169, 736–749.e18. <https://doi.org/10.1016/J.CELL.2017.04.016>.
107. Phillips, D., Matusiak, M., Gutierrez, B.R., Bhave, S.S., Barlow, G.L., Jiang, S., Demeter, J., Smythe, K.S., Pierce, R.H., Fling, S.P., et al. (2021). Immune cell topography predicts response to PD-1 blockade in cutaneous T cell lymphoma. *Nat. Commun.* 12, 6726. <https://doi.org/10.1038/s41467-021-26974-6>.
108. Moldoveanu, D., Ramsay, L.A., Lajoie, M., Anderson-Trocme, L., Lingrand, M., Berry, D., Perus, L.J.M., Wei, Y., Moraes, C., Alkallas, R., et al. (2022). Spatially mapping the immune landscape of melanoma using imaging mass cytometry. *Sci. Immunol.* 7, 5072. https://doi.org/10.1126/SCIMMUNOL.ABI5072/SUPPL_FILE/SCIMMUNOL.ABI5072_TABLES_S1.
109. Liudahl, S.M., Betts, C.B., Sivagnanam, S., Morales-Oyarvide, V., da Silva, A., Yuan, C., Hwang, S., Grossblatt-Wait, A., Leis, K.R., Larson, W., et al. (2021). Leukocyte heterogeneity in pancreatic ductal adenocarcinoma: phenotypic and spatial features associated with clinical outcome. *Cancer Discov.* 2020, 0841. <https://doi.org/10.1158/2159-8290.cd-20-0841>.
110. Zhu, Y., Ferri-Borgogno, S., Sheng, J., Yeung, T.L., Burks, J.K., Cappello, P., Jazaeri, A.A., Kim, J.H., Han, G.H., Birrer, M.J., et al. (2021). SIO: a spatioimageomics pipeline to identify prognostic biomarkers associated with the ovarian tumor microenvironment. *Cancers* 13, 1777. <https://doi.org/10.3390/CANCERS13081777>.
111. Keren, L., Bosse, M., Marquez, D., Angoshtari, R., Jain, S., Varma, S., Yang, S.-R., Kurian, A., van Valen, D., West, R., et al. (2018). A structured tumor-immune microenvironment in triple negative breast cancer revealed by multiplexed ion beam imaging. *Cell* 174, 1373–1387.e19. <https://doi.org/10.1016/J.CELL.2018.08.039>.
112. Jackson, H.W., Fischer, J.R., Zanotelli, V.R.T., Ali, H.R., Mechera, R., Soysal, S.D., Moch, H., Muenst, S., Varga, Z., Weber, W.P., and Bodenmiller, B. (2020). The single-cell pathology landscape of breast cancer. *Nature* 578, 615–620. <https://doi.org/10.1038/s41586-019-1876-x>.
113. Risom, T., Glass, D.R., Averbukh, I., Liu, C.C., Baranski, A., Kagel, A., McCaffrey, E.F., Greenwald, N.F., Rivero-Gutiérrez, B., Strand, S.H., et al. (2022). Transition to invasive breast cancer is associated with progressive changes in the structure and composition of tumor stroma. *Cell* 185, 299–310. <https://doi.org/10.1016/J.CELL.2021.12.023/ATTACHMENT/71EC6EB7-7D73-4460-B538-1E2D7805F52E/MMC5.XLSX>.
114. Svedlund, J., Strell, C., Qian, X., Zilkens, K.J.C., Tobin, N.P., Bergh, J., Sieuwerts, A.M., and Nilsson, M. (2019). Generation of *in situ* sequencing based OncoMaps to spatially resolve gene expression profiles of diagnostic and prognostic markers in breast cancer. *EBioMedicine* 48, 212–223. <https://doi.org/10.1016/J.EBIOM.2019.09.009>.
115. Aoki, T., Chong, L.C., Takata, K., Milne, K., Hav, M., Colombo, A., Chavéz, E.A., Nissen, M., Wang, X., Miyata-Takata, T., et al. (2020). Single-cell transcriptome analysis reveals disease-defining t-cell subsets in the tumor microenvironment of classic hodgkin lymphoma. *Cancer Discov.* 10, 406–421. <https://doi.org/10.1158/2159-8290.CD-19-0680-333427/AM/SINGLE-CELL-TRANSCRIPTOME-ANALYSIS-REVEALS-DISEASE>.
116. Nieto, P., Elosua-Bayes, M., Trincado, J.L., Marchese, D., Massoni-Badosa, R., Salvany, M., Henriquez, A., Nieto, J., Aguilar-Fernández, S., Mereu, E., et al. (2021). A single-cell tumor immune atlas for precision oncology. *Genome Res.* 31, 1913–1926. <https://doi.org/10.1101/GR.273300.120>.
117. Schapiro, D., Jackson, H.W., Raghuraman, S., Fischer, J.R., Zanotelli, V.R.T., Schulz, D., Giesen, C., Catena, R., Varga, Z., and Bodenmiller, B. (2017). histoCAT: analysis of cell phenotypes and interactions in multiplex image cytometry data. *Nat. Methods* 14, 873–876. <https://doi.org/10.1038/nmeth.4391>.
118. McCaffrey, E.F., Donato, M., Keren, L., Chen, Z., Delmastro, A., Fitzpatrick, M.B., Gupta, S., Greenwald, N.F., Baranski, A., Graf, W., et al. (2022). The immunoregulatory landscape of human tuberculosis granulomas. *Nat. Immunol.* 23, 318–329. <https://doi.org/10.1038/s41590-021-01121-x>.
119. Browaeys, R., Saelens, W., and Saeys, Y. (2019). NicheNet: modeling intercellular communication by linking ligands to target genes. *Nat. Methods* 17, 159–162. <https://doi.org/10.1038/s41592-019-0667-5>.
120. Dries, R., Zhu, Q., Dong, R., Eng, C.H.L., Li, H., Liu, K., Fu, Y., Zhao, T., Sarkar, A., Bao, F., et al. (2021). Giotto: a toolbox for integrative analysis and visualization of spatial expression data. *Genome Biol.* 22, 78. <https://doi.org/10.1186/S13059-021-02286-2>.
121. Bhave, S.S., Barlow, G.L., Schürch, C.M., and Nolan, G.P. (2022). Tissue schematics map the specialization of immune tissue motifs and their appropriation by tumors. *Cell Syst.* 13, 109–130.e6. <https://doi.org/10.1016/J.CELS.2021.09.012>.
122. Chen, Z., Soifer, I., Hilton, H., Keren, L., and Jojic, V. (2020). Modeling multiplexed images with spatial-LDA reveals novel tissue microenvironments. *J. Comput. Biol.* 27, 1204–1218. <https://doi.org/10.1089/CMB.2019.0340/ASSET/IMAGES/LARGE/CMB.2019.0340 FIGURE6.JPG>.
123. Danenberg, E., Bardwell, H., Zanotelli, V.R.T., Provenzano, E., Chin, S.F., Rueda, O.M., Green, A., Rakha, E., Aparicio, S., Ellis, I.O., et al. (2022). Breast tumor microenvironment structures are associated with genomic features and clinical outcome. *Nat. Genet.* 54, 660–669. <https://doi.org/10.1038/s41588-022-01041-y>.
124. Thrane, K., Eriksson, H., Maaskola, J., Hansson, J., and Lundeberg, J. (2018). Spatially resolved transcriptomics enables dissection of genetic heterogeneity in stage III cutaneous malignant melanoma. *Cancer Res.* 78, 5970–5979. <https://doi.org/10.1158/0008-5472.CAN-18-0747>.
125. Pelka, K., Hofree, M., Chen, J.H., Sarkizova, S., Pirl, J.D., Jorgji, V., Bejnood, A., Dionne, D., Ge, W.H., Xu, K.H., et al. (2021). Spatially organized multicellular immune hubs in human colorectal cancer. *Cell* 184, 4734–4752.e20. <https://doi.org/10.1016/J.CELL.2021.08.003>.
126. Berglund, E., Maaskola, J., Schultz, N., Friedrich, S., Marklund, M., Bergenstråhl, J., Tarish, F., Tanoglidli, A., Vickovic, S., Larsson, L., et al. (2018). Spatial maps of prostate cancer transcriptomes reveal an unexplored landscape of heterogeneity. *Nat. Commun.* 9, 2419–2513. <https://doi.org/10.1038/s41467-018-04724-5>.
127. Ali, H.R., Jackson, H.W., Zanotelli, V.R.T., Danenberg, E., Fischer, J.R., Bardwell, H., Provenzano, E., CRUK IMAXT Grand Challenge Team, Rueda, O.M., Chin, S.F., et al. (2020). Imaging mass cytometry and multi-platform genomics define the phenogenomic landscape of breast cancer. *Nat. Can. (Que.)* 1, 163–175. <https://doi.org/10.1038/s43018-020-0026-6>.
128. Hartmann, F.J., Mrdjen, D., McCaffrey, E., Glass, D.R., Greenwald, N.F., Bharadwaj, A., Khair, Z., Verberk, S.G.S., Baranski, A., Baskar, R., et al. (2021). Single-cell metabolic profiling of human cytotoxic T cells. *Nat. Biotechnol.* 39, 186–197. <https://doi.org/10.1038/s41587-020-06518>.
129. Wu, Y., Yang, S., Ma, J., Chen, Z., Song, G., Rao, D., Cheng, Y., Huang, S., Liu, Y., Jiang, S., et al. (2022). Spatiotemporal immune landscape of colorectal cancer liver metastasis at single-cell level. *Cancer Discov.* 12, 134–153. <https://doi.org/10.1158/2159-8290.CD-21-0316/673844/AM/SPATIOTEMPORAL-IMMUNE-LANDSCAPE-OF-COLORECTAL>.
130. Ji, A.L., Rubin, A.J., Thrane, K., Jiang, S., Reynolds, D.L., Meyers, R.M., Guo, M.G., George, B.M., Mollbrink, A., Bergenstråhl, J., et al. (2020). Multimodal analysis of composition and spatial architecture in human squamous cell carcinoma. *Cell* 182, 497–514.e22. <https://doi.org/10.1016/J.CELL.2020.05.039>.
131. Sautès-Fridman, C., Petitprez, F., Calderaro, J., and Fridman, W.H. (2019). Tertiary lymphoid structures in the era of cancer immunotherapy.

- Nat. Rev. Cancer 19, 307–325. <https://doi.org/10.1038/s41568-019-0144-6>.
132. Schumacher, T.N., and Thommen, D.S. (2022). Tertiary lymphoid structures in cancer. Science 1979, 375. <https://doi.org/10.1126/SCIENCE.ABF9419/ASSET/B44E9511-03AD-436A-89A0-110BDC25E3A7/ASSETS/IMAGES/LARGE/SCIENCE.ABF9419-F3.JPG>.
133. Meylan, M., Petitprez, F., Becht, E., Bougoün, A., Pupier, G., Calvez, A., Giglioli, I., Verkarre, V., Lacroix, G., Verneau, J., et al. (2022). Tertiary lymphoid structures generate and propagate anti-tumor antibody-producing plasma cells in renal cell cancer. Immunity 55, 527–541.e5. <https://doi.org/10.1016/J.IMMUNI.2022.02.001>.
134. Hoch, T., Schulz, D., Eling, N., Gómez, J.M., Levesque, M.P., and Bodenmiller, B. (2022). Multiplexed imaging mass cytometry of the chemokine milieu in melanoma characterizes features of the response to immunotherapy. Sci. Immunol. 7, 1692. https://doi.org/10.1126/SCIIIMMUNOL.ABK1692/SUPPL_FILE/SCIIMMUNOL.ABK1692_DATA_FILES_S1_AND_S2.ZIP.
135. Sade-Feldman, M., Yizhak, K., Bjørgaard, S.L., Ray, J.P., de Boer, C.G., Jenkins, R.W., Lieb, D.J., Chen, J.H., Frederick, D.T., Barzily-Rokni, M., et al. (2018). Defining T cell states associated with response to checkpoint immunotherapy in melanoma. Cell 175, 998–1013.e20. <https://doi.org/10.1016/J.CELL.2018.10.038>.
136. Danenberg, E., Bardwell, H., Zanotelli, V.R.T., Provenzano, E., Chin, S.F., Rueda, O.M., Green, A., Rakha, E., Aparicio, S., Ellis, I.O., et al. (2022). Breast tumor microenvironment structures are associated with genomic features and clinical outcome. Nat. Genet. 54, 660–669. <https://doi.org/10.1038/s41588-022-01041-y>.
137. Ali, H.R., Jackson, H.W., Zanotelli, V.R.T., Danenberg, E., Fischer, J.R., Bardwell, H., Provenzano, E., CRUK IMAXT Grand Challenge Team, Rueda, O.M., Chin, S.F., et al. (2020). Imaging mass cytometry and multiplatform genomics define the phenogenomic landscape of breast cancer. Nat. Can. (Que.) 1, 163–175. <https://doi.org/10.1038/s43018-020-0026-6>.
138. Jackson, H.W., Fischer, J.R., Zanotelli, V.R.T., Ali, H.R., Mehera, R., Soysal, S.D., Moch, H., Muenst, S., Varga, Z., Weber, W.P., and Bodenmiller, B. (2020). The single-cell pathology landscape of breast cancer. Nature 578, 615–620. <https://doi.org/10.1038/s41586-019-1876-x>.
139. Barkley, D., Moncada, R., Pour, M., Liberman, D.A., Dryg, I., Werba, G., Wang, W., Baron, M., Rao, A., Xia, B., et al. (2022). Cancer cell states recur across tumor types and form specific interactions with the tumor microenvironment. Nat. Genet. 54, 1192–1201. <https://doi.org/10.1038/s41588-022-01141-9>.
140. Maier, B., Leader, A.M., Chen, S.T., Tung, N., Chang, C., LeBerichel, J., Chudnovskiy, A., Maskey, S., Walker, L., Finnigan, J.P., et al. (2020). A conserved dendritic-cell regulatory program limits antitumour immunity. Nature 580, 257–262. <https://doi.org/10.1038/s41586-020-2134-y>.
141. Rovira-Clavé, X., Drainas, A.P., Jiang, S., Bai, Y., Baron, M., Zhu, B., Markovic, M., Coles, G.L., Bassik, M.C., Sage, J., et al. (2021). Spatial epitope barcoding reveals subclonal tumor patch behaviors. Preprint at bioRxiv. <https://doi.org/10.1101/2021.06.29.449991>.
142. Liu, H.C., Viswanath, D.I., Pesaresi, F., Xu, Y., Zhang, L., Di Trani, N., Paez-Mayorga, J., Hernandez, N., Wang, Y., Erm, D.R., et al. (2021). Potentiating antitumor efficacy through radiation and sustained intratumoral delivery of anti-CD40 and anti-PDL1. Int. J. Radiat. Oncol. Biol. Phys. 110, 492–506. <https://doi.org/10.1016/J.IJROBP.2020.07.2326>.
143. van Maldegem, F., Valand, K., Cole, M., Patel, H., Angelova, M., Rana, S., Colliver, E., Enfield, K., Bah, N., Kelly, G., et al. (2021). Characterisation of tumour microenvironment remodelling following oncogene inhibition in preclinical studies with imaging mass cytometry. Nat. Commun. 12, 5906–5914. <https://doi.org/10.1038/s41467-021-26214-x>.
144. Shekarian, T., Zinner, C.P., Bartoszek, E.M., Duchemin, W., Wachnowicz, A.T., Hogan, S., Etter, M.M., Flammer, J., Paganetti, C., Martins, T.A., et al. (2022). Immunotherapy of glioblastoma explants induces interferon- γ responses and spatial immune cell rearrangements in tumor center, but not periphery. Sci. Adv. 8, 9440. <https://doi.org/10.1126/SCIAADV.ABN9440>.
145. Patwa, A., Yamashita, R., Long, J., Risom, T., Angelo, M., Keren, L., and Rubin, D.L. (2021). Multiplexed imaging analysis of the tumor-immune microenvironment reveals predictors of outcome in triple-negative breast cancer. Commun. Biol. 4, 852–914. <https://doi.org/10.1038/s42003-021-02361-1>.
146. Lu, S., Stein, J.E., Rimm, D.L., Wang, D.W., Bell, J.M., Johnson, D.B., Sosman, J.A., Schalper, K.A., Anders, R.A., Wang, H., et al. (2019). Comparison of biomarker modalities for predicting response to PD-1/PD-L1 checkpoint blockade: a systematic review and meta-analysis. JAMA Oncol. 5, 1195–1204. <https://doi.org/10.1001/JAMAONCOL.2019.1549>.
147. Tumeh, P.C., Harview, C.L., Yearley, J.H., Shintaku, I.P., Taylor, E.J.M., Robert, L., Chmielowski, B., Spasic, M., Henry, G., Ciobanu, V., et al. (2014). PD-1 blockade induces responses by inhibiting adaptive immune resistance. Nature 515, 568–571. <https://doi.org/10.1038/nature13954>.
148. Petitprez, F., de Reyniès, A., Keung, E.Z., Chen, T.W.W., Sun, C.M., Calderaro, J., Jeng, Y.M., Hsiao, L.P., Lacroix, L., Bougoün, A., et al. (2020). B cells are associated with survival and immunotherapy response in sarcoma. Nature 577, 556–560. <https://doi.org/10.1038/s41586-019-1906-8>.
149. Sautès-Fridman, C., Lawand, M., Giraldo, N.A., Kaplon, H., Germain, C., Fridman, W.H., and Dieu-Nosjean, M.C. (2016). Tertiary lymphoid structures in cancers: prognostic value, regulation, and manipulation for therapeutic intervention. Front. Immunol. 7, 407. <https://doi.org/10.3389/FIMMU.2016.00407>.
150. Cabrita, R., Lauss, M., Sanna, A., Donia, M., Skaarup Larsen, M., Mitra, S., Johansson, I., Phung, B., Harbst, K., Vallon-Christersson, J., et al. (2020). Tertiary lymphoid structures improve immunotherapy and survival in melanoma. Nature 577, 561–565. <https://doi.org/10.1038/s41586-019-1914-8>.
151. Di Caro, G., Bergomas, F., Grizzi, F., Doni, A., Bianchi, P., Malesci, A., Lahgi, L., Allavena, P., Mantovani, A., and Marchesi, F. (2014). Occurrence of tertiary lymphoid tissue is associated with T-cell infiltration and predicts better prognosis in early-stage colorectal cancers. Clin. Cancer Res. 20, 2147–2158. <https://doi.org/10.1158/1078-0432.CCR-13-2590>.
152. Helmink, B.A., Reddy, S.M., Gao, J., Zhang, S., Basar, R., Thakur, R., Yizhak, K., Sade-Feldman, M., Blando, J., Han, G., et al. (2020). B cells and tertiary lymphoid structures promote immunotherapy response. Nature 577, 549–555. <https://doi.org/10.1038/s41586-019-1922-8>.
153. Almogy, G., Pratt, M., Oberstrass, F., Lee, L., Mazur, D., Beckett, N., Barad, O., Soifer, I., Perelman, E., Etzioni, Y., et al. (2022). Cost-efficient whole genome-sequencing using novel mostly natural sequencing-by-synthesis chemistry and open fluidics platform. Preprint at bioRxiv. <https://doi.org/10.1101/2022.05.29.493900>.
154. Lin, J.R., Fallahi-Sichani, M., Chen, J.Y., and Sorger, P.K. (2016). Cyclic immunofluorescence (CycIF), A highly multiplexed method for single-cell imaging. Curr. Protoc. Chem. Biol. 8, 251–264. <https://doi.org/10.1002/CPCH.14>.
155. Baranski, A., Milo, I., Greenbaum, S., Oliveria, J.P., Mrdjén, D., Angelo, M., and Keren, L. (2021). MAUI (MBI analysis user interface)—an image processing pipeline for multiplexed mass based imaging. PLoS Comput. Biol. 17, e1008887. <https://doi.org/10.1371/JOURNAL.PCB.1008887>.
156. Chevrier, S., Crowell, H.L., Zanotelli, V.R.T., Engler, S., Robinson, M.D., and Bodenmiller, B. (2018). Compensation of signal spillover in suspension and imaging mass cytometry. Cell Syst. 6, 612–620.e5. <https://doi.org/10.1016/J.CELLS.2018.02.010>.
157. Taube, J.M., Akturk, G., Angelo, M., Engle, E.L., Gnjatic, S., Greenbaum, S., Greenwald, N.F., Hedvat, C.V., Hollmann, T.J., Juco, J., et al. (2020). The Society for Immunotherapy of Cancer statement on best practices for multiplex immunohistochemistry (IHC) and immunofluorescence (IF) staining and validation. J. Immunother. Cancer 8, e000155. <https://doi.org/10.1136/JITC-2019-000155>.
158. Han, G., Chen, S.Y., Gonzalez, V.D., Zunder, E.R., Fanti, W.J., and Nolan, G.P. (2017). Atomic mass tag of bismuth-209 for increasing the immunoassay multiplexing capacity of mass cytometry. Cytometry A. 91, 1150–1163. <https://doi.org/10.1002/CYTO.A.23283>.
159. Cleary, B., Simonton, B., Bezney, J., Murray, E., Alam, S., Sinha, A., Habibi, E., Marshall, J., Lander, E.S., Chen, F., and Regev, A. (2021). Compressed sensing for highly efficient imaging transcriptomics. Nat. Biotechnol. 39, 936–942. <https://doi.org/10.1038/s41587-021-00883-x>.

160. Shi, L., Wei, M., Miao, Y., Qian, N., Shi, L., Singer, R.A., Benninger, R.K.P., and Min, W. (2021). Highly-multiplexed volumetric mapping with Raman dye imaging and tissue clearing. *Nat. Biotechnol.* 40, 364–373. <https://doi.org/10.1038/s41587-021-01041-z>.
161. Kuett, L., Catena, R., Özcan, A., Plüss, A., Cancer Grand Challenges IMAXT Consortium, Schraml, P., Moch, H., de Souza, N., Bodenmiller, B., Balasubramanian, S., et al. (2021). Three-dimensional imaging mass cytometry for highly multiplexed molecular and cellular mapping of tissues and the tumor microenvironment. *Nat. Can. (Que.)* 3, 122–133. <https://doi.org/10.1038/s43018-021-00301-w>.
162. Janai, J., Güney, F., Behl, A., and Geiger, A. (2020). Computer vision for autonomous vehicles: problems, datasets and state of the art. *FNT. in Computer Graphics and Vision* 12, 1–308. <https://doi.org/10.1561/0600000079>.
163. Adjabi, I., Ouahabi, A., Benzaoui, A., and Taleb-Ahmed, A. (2020). Past, present, and future of face recognition: a review. *Electronics* 9, 1188. <https://doi.org/10.3390/ELECTRONICS9081188>.
164. Liu, C., Hirota, K., Ma, J., Jia, Z., and Dai, Y. (2021). Facial expression recognition using hybrid features of pixel and geometry. *IEEE Access* 9, 18876–18889. <https://doi.org/10.1109/ACCESS.2021.3054332>.
165. Kalinin, S.V., Ophus, C., Voyles, P.M., Erni, R., Kepaptsoglou, D., Grillo, V., Lupini, A.R., Oxley, M.P., Schwenker, E., Chan, M.K.Y., et al. (2022). Machine learning in scanning transmission electron microscopy. *Nat. Rev. Methods Primers* 2, 11–28. <https://doi.org/10.1038/s43586-022-00095-w>.
166. Esteva, A., Chou, K., Yeung, S., Naik, N., Madani, A., Mottaghi, A., Liu, Y., Topol, E., Dean, J., and Socher, R. (2021). Deep learning-enabled medical computer vision. *NPJ Digit. Med.* 4, 5–9. <https://doi.org/10.1038/s41746-020-00376-2>.
167. Fu, Y., Jung, A.W., Torne, R.V., Gonzalez, S., Vöhringer, H., Shmatko, A., Yates, L.R., Jimenez-Linan, M., Moore, L., and Gerstung, M. (2020). Pan-cancer computational histopathology reveals mutations, tumor composition and prognosis. *Nat. Can. (Que.)* 1, 800–810. <https://doi.org/10.1038/s43018-020-0085-8>.
168. Amitay, Y., Bussi, Y., Feinstein, B., Bagon, S., Milo, I., and Keren, L. (2022). CellSighter – a neural network to classify cells in highly multiplexed images. Preprint at bioRxiv. <https://doi.org/10.1101/2022.11.07.515441>.
169. Schapiro, D., Yapp, C., Sokolov, A., Reynolds, S.M., Chen, Y.A., Sudar, D., Xie, Y., Muhlich, J., Arias-Camison, R., Arena, S., et al. (2022). MITI minimum information guidelines for highly multiplexed tissue images. *Nat. Methods* 19, 262–267. <https://doi.org/10.1038/s41592-022-01415-4>.
170. Manz, T., Gold, I., Patterson, N.H., McCallum, C., Keller, M.S., Herr, B.W., Börner, K., Spraggins, J.M., and Gehlenborg, N. (2022). Viv: multi-scale visualization of high-resolution multiplexed bioimaging data on the web. *Nat. Methods* 19, 515–516. <https://doi.org/10.1038/s41592-022-01482-7>.
171. Regev, A., Teichmann, S., Rozenblatt-Rosen, O., Stubbington, M., Ardlie, K., Amit, I., Arlotta, P., Bader, G., Benoist, C., Biton, M., et al. (2018). The human cell atlas white paper. Preprint at arXiv. <https://doi.org/10.48550/arxiv.1810.05192>.
172. Rozenblatt-Rosen, O., Regev, A., Oberdoerffer, P., Nawy, T., Hupalowska, A., Rood, J.E., Ashenberg, O., Cerami, E., Coffey, R.J., Demir, E., et al. (2020). The human tumor atlas network: charting tumor transitions across space and time at single-cell resolution. *Cell* 181, 236–249. <https://doi.org/10.1016/J.CELL.2020.03.053>.
173. HubMAP Consortium (2019). The human body at cellular resolution: the NIH Human Biomolecular Atlas Program. *Nature* 574, 187–192. <https://doi.org/10.1038/s41586-019-1629-x>.
174. Deng, Y., Bartosovic, M., Ma, S., Zhang, D., Kukanja, P., Xiao, Y., Su, G., Liu, Y., Qin, X., Rosoklja, G.B., et al. (2022). Spatial profiling of chromatin accessibility in mouse and human tissues. *Nature* 609, 375–383. <https://doi.org/10.1038/s41586-022-05094-1>.
175. Deng, Y., Bartosovic, M., Kukanja, P., Zhang, D., Liu, Y., Su, G., Enninfoul, A., Bai, Z., Castelo-Branco, G., and Fan, R. (2022). Spatial-CUT&Tag: spatially resolved chromatin modification profiling at the cellular level. *Science* 375, 681–686. https://doi.org/10.1126/SCIENCE.ABG7216/SUPPL_FILE/SCIENCE.ABG7216_MDAR_REPRODUCIBILITY_CHECK_LIST.PDF.
176. Zeng, H., Huang, J., Ren, J., Wang, C.K., Tang, Z., Zhou, Y., Aditham, A., Shi, H., Sui, X., and Wang, X. (2022). Spatially resolved single-cell transcriptomics at molecular resolution. Preprint at bioRxiv. <https://doi.org/10.1101/2022.09.27.509605>.
177. Jiang, S., Chan, C.N., Rovira-Clavé, X., Chen, H., Bai, Y., Zhu, B., McCaffrey, E., Greenwald, N.F., Liu, C., Barlow, G.L., et al. (2022). Combined protein and nucleic acid imaging reveals virus-dependent B cell and macrophage immunosuppression of tissue microenvironments. *Immunity* 55, 1118–1134.e8. <https://doi.org/10.1016/J.IMMUNI.2022.03.020>.
178. Todhunter, M.E., Jee, N.Y., Hughes, A.J., Coyle, M.C., Cerchiari, A., Farlow, J., Garbe, J.C., LaBarge, M.A., Desai, T.A., and Gartner, Z.J. (2015). Programmed synthesis of three-dimensional tissues. *Nat. Methods* 12, 975–981. <https://doi.org/10.1038/NMETH.3553>.
179. Chao, G., Wannier, T.M., Gutierrez, C., Borders, N.C., Appleton, E., Chadha, A., Lebar, T., and Church, G.M. (2022). helixCAM: a platform for programmable cellular assembly in bacteria and human cells. *Cell* 185, 3551–3567.e39. <https://doi.org/10.1016/J.CELL.2022.08.012>.
180. Gracia Villacampa, E., Larsson, L., Mirzazadeh, R., Kvastad, L., Ander-son, A., Mollbrink, A., Kokaraki, G., Monteil, V., Schultz, N., Appelberg, K.S., et al. (2021). Genome-wide spatial expression profiling in formalin-fixed tissues. *Cell Genomics* 1, 100065. <https://doi.org/10.1016/J.XGEN.2021.100065>.
181. Lim, S.M., Pyo, K.H., Soo, R.A., and Cho, B.C. (2021). The promise of bispecific antibodies: clinical applications and challenges. *Cancer Treat Rev.* 99, 102240. <https://doi.org/10.1016/J.CTRV.2021.102240>.